

USING WISE TO FIND OBSCURED AGN ACTIVITY IN  
SDSS MERGERS AND INTERACTIONS

A THESIS IN  
Physics and Astronomy

Presented to the Faculty of the University  
of Missouri-Kansas City in partial fulfillment of  
the requirements for the degree

MASTER OF SCIENCE

by  
MADALYN ELIZABETH WESTON

B.S., Missouri University of Science and Technology, 2012

Kansas City, Missouri  
2015



USING WISE TO FIND OBSCURED AGN ACTIVITY IN  
SDSS MERGERS AND INTERACTIONS

Madalyn Elizabeth Weston, Candidate for the Master of Science Degree

University of Missouri – Kansas City, 2015

ABSTRACT

In simulations, major encounters between gas-rich galaxies are predicted to drive gas to the centers of interacting and merging systems triggering new star formation (SF) and fueling an active galactic nucleus (AGN). Depending on the rate of SF, large amounts of obscuring dust can make detection of merger-induced activity difficult and may be at the heart of the ongoing merger-AGN connection debate. To provide better constraints on the importance of obscured AGNs, we use data from the Wide-field Infrared Survey Explorer (WISE) for a comprehensive sample of over 1000 major galaxy interactions and ongoing mergers visually selected from the SDSS with  $10^{10} M_{\odot}$  and  $0.01 < z < 0.08$ . We examine the [3.4]-[4.6] versus [4.6]-[12] color-color plane and find that most interactions and mergers have the same colors as “normal” (non-interacting and non-merging) galaxies, which define a narrow [3.4]-[4.6] locus and span a wide range in [4.6]-[12] colors from spectroscopically quiescent (blue, no warm dust) to galaxies with obscured SF. We find that 2 – 9 percent of mergers (and 1.0 – 2.5 percent of interactions) have unusually red [3.4]-[4.6] colors, which

are associated with dust-obscured (Type-2) AGNs. Mergers (interactions) are 5 – 18 (3 – 5) times more likely to host a buried AGN than normal galaxies. This increased likelihood of dusty AGN activity in mergers and interactions supports an AGN-merger connection. We investigate the nature of merging and interacting galaxies with dusty AGN. We find that dusty AGN mergers and interactions favor smaller pair separations, smaller dark matter halo masses, and higher [OIII] luminosities (a proxy for AGN power) than the bulk of mergers and interactions with normal WISE colors. Using SDSS  $urz$  colors to distinguish quiescent from star-forming galaxies, we find that more than three-quarters of the WISE AGN subpopulation of mergers and interactions are forming stars. We find that AGNs also classified as ongoing mergers are 2 – 6 times more likely to be obscured than AGNs in non-merging, non-interacting galaxies. Around half of merging AGNs are obscured, suggesting that shorter wavelengths will be inadequate in selecting AGNs in merging systems. We find no association between merging systems and optically identified AGNs (Seyferts), suggesting that central star formation (and thus dust obscuration) is the key to making an AGN in a merger. Our findings indicate a strong association between ongoing star formation and dust-enshrouded black hole growth in merging galaxies as predicted in the modern merger hypothesis.



## APPROVAL PAGE

The faculty listed below, appointed by the Dean of the College of Arts and Sciences have examined a thesis titled “Using WISE to Find Obscured AGN Activity in SDSS Mergers and Interactions,” presented by Madalyn Elizabeth Weston, candidate for the Master of Science degree, and certify that in their opinion it is worthy of acceptance.

### Supervisory Committee

Daniel McIntosh, Ph.D., Committee Chair  
Department of Physics and Astronomy

Mark Brodwin, Ph.D.  
Department of Physics and Astronomy

Elizabeth Stoddard, Ph.D.  
Department of Physics and Astronomy

## TABLE OF CONTENTS

ABSTRACT .....	iii
LIST OF ILLUSTRATIONS .....	viii
LIST OF TABLES .....	x
ACKNOWLEDGEMENTS .....	xi
Chapter	
1 INTRODUCTION .....	1
2 SAMPLE DESCRIPTION .....	8
2.1 Mergers and Interactions from the SDSS .....	8
2.2 SDSS Spectroscopic Emission Types .....	12
2.3 WISE Photometry .....	16
3 WISE COLOR ANALYSIS .....	21
3.1 WISE Colors for Spectroscopic Types .....	21
3.2 Incidence of Dusty AGNs in Mergers and Interactions .....	30
4 NATURE OF WISE AGN .....	33
4.1 Galaxy and Pair Properties .....	34
4.2 Group Properties .....	39
4.3 [OIII] Luminosity as an Indicator of AGN Power .....	41
4.4 Star Formation of the Host Galaxy .....	44
5 DISCUSSION .....	48
5.1 The Dusty AGN-Merger Connection .....	48
5.2 Star Formation in Dusty AGN Mergers .....	55

5.3 Properties of WISE AGN Mergers and Interactions.....	56
6 SUMMARY .....	60
Appendix	
THE AFFECT OF SMALL NUMBER ON KOLMOGOROV-SMIRNOV (K-S)	
TWO-SAMPLE TESTS.....	62
REFERENCE LIST .....	67
VITA.....	73

## LIST OF ILLUSTRATIONS

Figure		Page
1	The Major Merger Model by Hopkins et al. (2008).....	4
2	Example of Galaxies in the Merging and Interacting Sample .....	10
3	Mass Ratio and Stellar Mass for Merging and Interacting Sample.....	12
4	BPT Diagram for Merging and Interacting Galaxies.....	14
5	Example of SDSS Spectroscopy for Different Spectroscopic Types .....	15
6	Separation of Coordinates vs. Separation of Pair for Interactions .....	17
7	Example of Galaxies Removed from the WISE Sample .....	19
8	Example of Interactions Reclassified as Mergers for WISE Analysis.....	20
9	WISE Colors for Spectroscopic Types .....	23
10	Galaxy Spectral Energy Distribution (SED).....	24
11	WISE Colors for 42,655 Control Galaxies.....	29
12	WISE Colors for Merging and Interacting Galaxies.....	30
13	WISE Colors for Merging and Interacting Subsamples.....	34
14	Distributions of Mass, Mass Ratio, and Pair Separation for Mergers and Interactions .....	35
15	Distributions of Halo Mass for Mergers and Interactions .....	40
16	Distribution of [OIII] Luminosity for Merging and Interacting AGNs .....	43
17	SDSS urz Color-Plot for Mergers and Interactions .....	45
18	WISE AGN Mergers and Interactions .....	47
19	Examples of Misclassified Control Galaxies in the WISE AGN Population .....	53
20	Sample of Gaussian Distributions Used to Quantify the Affect of Small Numbers on K-S Test p-values.....	63
21	Distributions of p-values for Similar Distributions .....	64

22	Distributions of p-values for Different Distributions.....	66
----	--	----

## LIST OF TABLES

Table		Page
1	Example from the Catalogue of Merging and Interacting Systems.....	11
2	WISE Living Spaces of Spectroscopic Types .....	25
3	WISE AGN Fractions for Spectroscopic Subsample of High-Mass SDSS Galaxies .....	27
4	WISE AGN Fractions for Mergers and Interactions.....	31
5	K-S Test P-Values as a Proxy for Dusty AGN and Galaxy Property Relations.....	36
6	Obscuration Fractions for Galaxy Morphologies .....	50
7	Merging and Interacting Fractions in AGN Populations .....	51
8	WISE Color Analysis of Mergers and Interactions with urz-Selected Star Formation .....	55

## ACKNOWLEDGEMENTS

M.E.W. and D.H.M. thankfully acknowledge support from NASA grant NNX13AE96G and the Missouri Space Grant Consortium.

This publication makes use of data products from the Wide-field Infrared Survey Explorer, which is a joint project of the University of California, Los Angeles, and the Jet Propulsion Laboratory/California Institute of Technology, funded by the National Aeronautics and Space Administration.

M.E.W. would like to thank her committee for their advice and support throughout her time at UMKC.

She would also like to thank her family and friends for their love and encouragement.

Special Thanks to  
Dr. Jane Rigby (NASA Goddard)  
Xiachang Her (UMKC)  
Bandon Decker (UMKC)

# CHAPTER 1

## INTRODUCTION

A connection between major galaxy mergers and active galactic nuclei (AGNs) remains a debate in galaxy evolution research. Simulations of major galaxy mergers predict a heightened amount of black hole activity and star formation (Hopkins et al. 2008, Springel et al. 2005, DeBuhr et al. 2011, Volonteri et al. 2003). Many observational studies support the correlation between AGNs and merging systems (Karouzos et al. 2010, Treister et al. 2012, Ellison et al. 2013, Cotini et al. 2013, Rosario et al. 2015, Nazaryan et al. 2014, Satyapal et al. 2014). However, several researchers, particularly those working at shorter wavelengths, do not find such a connection (Villforth et al. 2014, Cisternas et al. 2011, Scott & Kaviraj 2014, Fan et al. 2014). One possible reason for this debate is dust obscuration caused by star formation (SF) in the center of some merging systems (Goulding et al. 2009), indicating that longer wavelengths, such as the infrared, may be able to provide a better understanding of the AGN-merger connection.

In the larger context of galaxy evolution, there are many compelling reasons to expect a connection between major gas-rich mergers and supermassive black hole (SMBH) growth. The hierarchical assembly of massive structures is a key feature of  $\Lambda$ CDM cosmology (White & Rees 1978). The growth of large-scale structures is predicted to drive galaxy mergers (Kauffmann et al. 1993, Baugh et al. 1996, Cole et al. 2000), which in turn have long been tied to the formation of galactic bulges and spheroidal galaxies (Lake & Dressler 1986, Shier & Fischer 1998, Rothberg & Joseph 2006). The masses of galaxy spheroids are strongly correlated with the masses of their SMBHs (Kauffmann & Haehnelt 2000).



Moreover, massive, bulge-dominated galaxies are predominantly passive and old (Kauffmann et al. 2003) requiring one or more processes to shutdown star production and maintain SF quenching. An oft-cited theoretical quenching process is AGN feedback (Kauffmann et al. 2003, Di Matteo et al. 2005, Schawinski et al. 2007, 2009, Kaviraj et al. 2011, McIntosh et al. 2014), which is the release of energy from black hole accretion, either through gas outflows (Granato et al. 2004) typically caused with gas-rich mergers (Di Matteo et al. 2005, Springel et al. 2005, Hopkins et al. 2006), or heating of the interstellar medium (Hopkins & Elvis 2010). Such feedback is especially important if gas-rich mergers trigger new strong SF activity as simulations predict (Hopkins et al. 2008, Kauffmann & Haehnelt 2000, Di Matteo et al. 2005, Springel et al. 2005).

All of the above has been neatly folded into the modern merger hypothesis and nicely summarized by Hopkins et al. (2008). Briefly, Hopkins et al. (2008) produced the following gas-rich major-merger model, in which quasar activity from  $z = 0 - 6$  was accurately reproduced through the merger process. First, two equal-mass, gas-rich galaxies pass one another, causing morphological disturbances, such as tidal tails, and causing a small rise in star formation (“interacting” phase). As the galaxies are gravitationally pulled back into one another, the gas inflows trigger both star formation and black hole growth (Hann et al. 2009), with the rates of both limited by the inflow of gas from the merger (“ongoing merger” phase, Kennicutt 1998). As the gas supply is used by star formation and black hole accretion in this coalescence, it will shroud the center of the merger with large obscuring columns of dust. When the gas supply is terminated, a brief unobscured quasar phase (Storchi-Bergmann et al. 2001, Schawinski et al. 2009) will be followed by a halt in the black hole accretion and a dead quasar is left over. Over time, the merger remnant will evolve into a spheroid or, if the

gas content in the surrounding halo is still high enough for star formation, a spheroidal disk (Barnes 2002, Springel & Hernquist 2005, Hopkins et al. 2009). An illustration of this complex process from Hopkins et al. (2008) is shown in Figure 1. The images around the sides of the figure demonstrate the physical nature of the merger at a given phase. The plot shows the changes in star formation (top) and AGN activity (bottom) relative to the timescale of the merger. As can be seen in the plot, there are two distinct phases containing a rise in the star formation and black hole activity: the Interaction/”Merger” stage, which we will refer to as the Interaction phase; and the combined Coalescence/(U)LIRG and Blowout stages, which combined we will refer to as the Merger phase. These two phases are predicted to be the most likely stages for detecting both star formation and AGN activity.

The connection to AGN activity predicted by simulations is supported by many studies that find high incidences of tidal features associated with AGNs (Treister et al. 2012, Ellison et al. 2013, Cotini et al. 2013, Rosario et al. 2015, Satyapal et al. 2014), including Karouzos et al. (2010), who found that nearly 30 percent of the active galaxies showed signs of an interaction or merger in the optical and infrared. Nazaryan et al. (2014) performed an optical study on 180 Markarian galaxy pairs and found that ongoing mergers are 7 times more likely to be an AGN than interacting pairs. In addition, AGN activity increased with decreasing pair separation. Satyapal et al. (2014) used a WISE color-color cut to find that 9 percent of ongoing mergers and 1 percent of interacting pairs in a redshift range  $z < 0.2$  are AGNs. Their control population in the same redshift range was found to be 0.5 percent obscured AGNs.

While simulations and many observational studies find a link between merging systems and AGNs, the topic is still a debate. Many studies, especially those in the X-ray

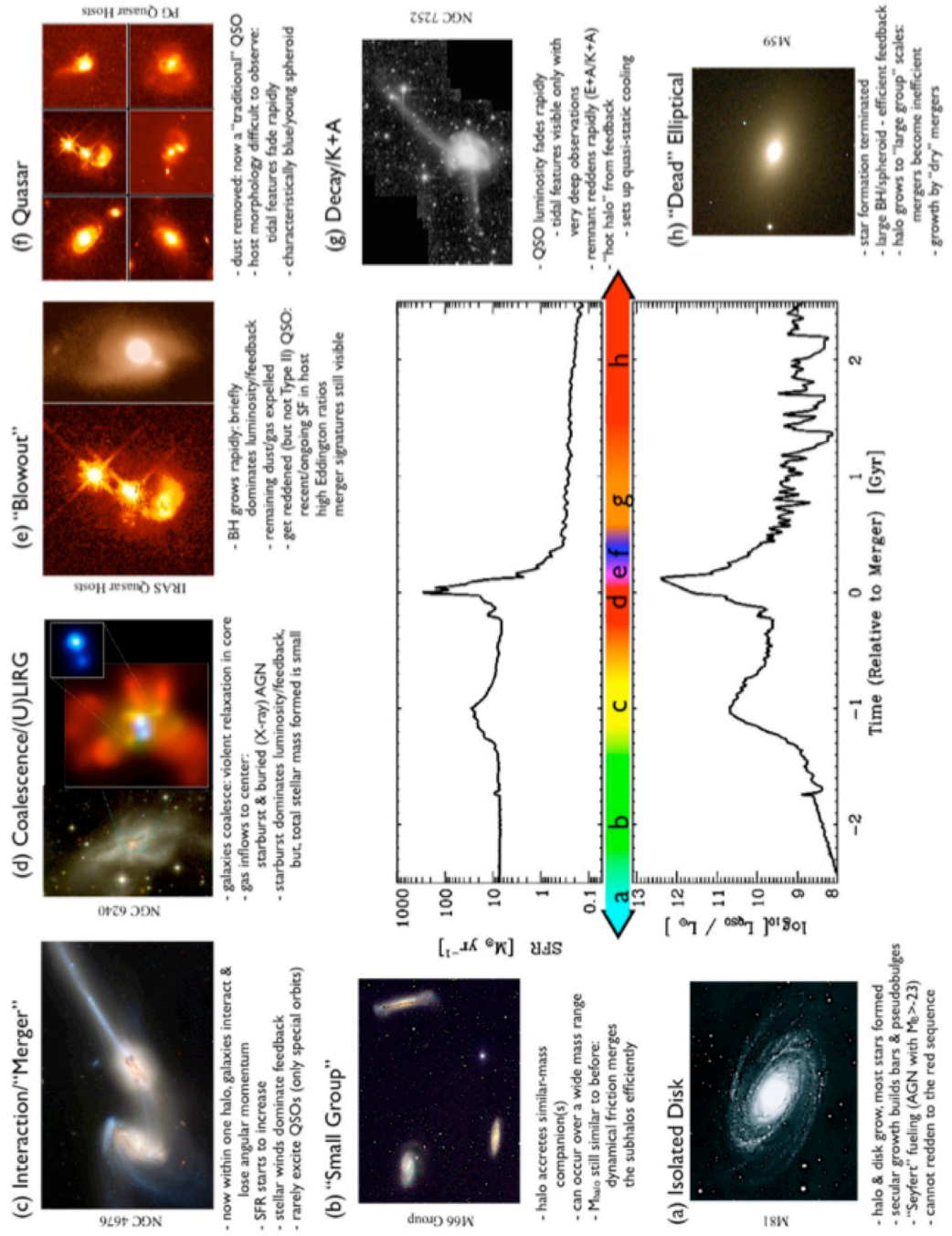


Figure 1. The Major Merger Model by Hopkins et al. (2008)  
 Source. Hopkins et al. (2008), NOAO/AURA/NSF

regime, do not find a correlation between mergers and AGN activity (Villforth et al. 2014, Cisternas et al. 2011, Scott & Kaviraj 2014, Fan et al. 2014). Villforth et al. (2014) studied the morphologies of 60 X-ray AGNs with  $0.5 < z < 0.8$  and found that, compared to a simulated control, AGN host galaxies showed no increase in asymmetries or disturbances. Their sample showed a maximum of 6 percent of AGNs were related to a major merger. In stark contrast to the simulation-predicted AGN-merger connection, Scott & Kaviraj (2014) used optical data to analyze Seyfert fraction as a function of pair separation in an interacting sample. They found a decrease in Seyferts as pair separation dropped, indicating a drop in AGN activity as interactions begin to merge. The majority of connection-lacking studies in the X-ray and optical regimes all suffer from one important implication of the simulation: dust obscuration caused by star formation in the nucleus.

The relationship between star formation and interacting systems is a well-documented phenomenon (Kennicutt et al. 1987, Barton et al. 2000, Lambas et al. 2003, Alonso et al. 2004, Ellison et al. 2008, Ellison et al. 2011). The tidal forces in the interaction funnel cold gas to the center of the merging system, which collapses into stellar nurseries. Star formation has been found to increase with decreasing pair separations in interacting pairs with  $d_{\text{sep}} \leq 150 h^{-1} \text{kpc}$  (Patton et al. 2013). Dust is produced in stellar nurseries and distributed through the interstellar medium via two mechanisms: AGB (Asymptotic Giant Branch) stars and supernovae (Clemens et al. 2013). As these methods would imply, the star formation rate in galaxies correlates to cold dust mass; the more star formation, the more dust in the galaxy. A large portion of a galaxy's bolometric luminosity can be absorbed by this dust and re-emitted in the infrared (Kennicutt 1998).

The addition of dust from star formation in a merging system can make AGNs hard to detect. Optical spectroscopic surveys can miss as much as half of the AGN population due to obscuration, particularly that caused by dust from star formation (Goulding et al. 2009). As the simulations predict (Hopkins et al. 2006, Hopkins et al. 2008, Springel et al. 2005, DeBuhr et al. 2011), star formation occurring in the center of a merging galaxy may also produce large obscuring columns, which limit the detection of the AGN. Because of this obscuration, shorter wavelength regimes can be ineffective at isolating obscured AGNs. Goulding et al. (2011) find that  $\approx 43 \pm 21$  percent of the AGN population are Compton-thick, and therefore too heavily obscured for X-ray detection. Further investigation of Compton-thick AGNs reveals a correlation to star formation and disturbed morphologies (Goulding et al. 2012). The likelihood of dust obscuration from increased star formation in merging and interacting systems leads to the use of the infrared wavelength regime to isolate AGNs, as countless other studies have done (Goulding et al. 2009, Stern et al. 2005, Stern et al. 2012, Assef et al. 2013, Yan et al. 2013, Jarrett et al. 2011).

Using the infrared in this study allows us to quantify the number of AGNs in merging and interacting systems. Using a sample of interacting and ongoing mergers visually selected from a large parent catalog of  $\sim 65,000$  SDSS (Sloan Digital Sky Survey) galaxies described in McIntosh et al. (2014), combined with mid-infrared colors from the Wide-Field Survey Explorer (WISE) All-Sky survey, we isolate a previously unclassified population of dusty AGNs and relate their relative frequency to that of a control sample to add support to the AGN-merger connection. We also analyze the properties of the infrared-selected AGNs to pinpoint any unique trends. In Chapter 2, we describe our sample of merging and interacting galaxies. In Chapter 3, we show our analysis and highlight the results of different WISE

color-color methods to select AGNs. We give a summary of WISE AGN properties for our interacting and merging sample in Chapter 4. We provide an overall summary of our results and how they compare to literature in Chapters 5 and 6. Throughout this paper, we assume a  $\Lambda$ CDM cosmological model with  $\Omega_m = 0.3$ ,  $\Omega_\Lambda = 0.7$ , and a Hubble constant of  $H_0 = 70 \text{ km s}^{-1}\text{Mpc}^{-1}$ .

## CHAPTER 2

### SAMPLE DESCRIPTION

As discussed in the Introduction, high levels of central obscuration in major mergers and galaxy-galaxy interactions can make it difficult to detect the presence of an AGN in ultraviolet or optical wavelengths. To search for obscured AGNs in a complete sample of visually selected major mergers and interactions from the SDSS, we use near- and mid-infrared data from the Wide-Field Survey Explorer (WISE) All-Sky Survey (Wright et al. 2010). WISE provides all-sky coverage at wavelengths between 3 and 22 microns with sensitivities better than IRAS and DIRBE, making it the best database to look for obscured AGNs in SDSS galaxies. Here, we describe our sample selection and provide details about the SDSS and WISE data we employ in our analysis.

#### **2.1 Mergers and Interactions from the SDSS**

For this paper, we focus on a sample of 1125 major galaxy-galaxy interactions and 100 ongoing merger (“train wreck”) galaxies with stellar masses greater than  $2 \times 10^{10} M_{\odot}$  and redshifts  $0.01 \leq z \leq 0.08$ . This sample is visually classified from a parent catalog of 63,454 SDSS DR4 galaxies taken from the New York University Value-Added Galaxy Catalog (NYU-VAGC, Blanton et al. 2005) reprocessing of the SDSS DR4 (Adelman-McCarthy et al. 2006) Main galaxy sample (Strauss et al. 2002) selection of spectroscopic targets with  $r(\text{AB}) \leq 17.77$  mag. Stellar masses for this catalog were calculated using stellar mass-to-light ratios from Bell et al. (2003), as described in detail in McIntosh et al. (2014).

The merger and interaction sample selection and classification criteria are described in detail in McIntosh et al. (in prep). Briefly, each galaxy in the parent catalog was examined

by D.H.M. and three students and classified as non-interacting, interacting, or merging. Examples of the sample are shown in Figure 2 and their catalog entries are given in Table 1. Ongoing mergers are defined as isolated and highly disturbed galaxies showing strong morphological signatures consistent with the recent merging or coalescence of two galaxies, such as tidal tails or loops, asymmetrical dust lanes, or double nuclei. Interacting galaxies are those found in pairs, with morphological disturbances such as tidal arms, warped disks, or bridges, identified in one or both galaxies. Projected separations for the pairs were calculated using the angular diameter distance equation

$$d_A = \frac{d_{sep}}{\delta\theta} = \frac{d_p}{1+z} \quad (1),$$

where  $d_A$  is the angular diameter distance to the pair,  $d_{sep}$  is the projected separation between the pair galaxies,  $\delta\theta$  is the angular separation between the pair galaxies,  $d_p$  is the proper distance to the pair, and  $z$  is the redshift of the pair (Ryden 2003). The pairs used in this sample were selected to have a projected separation  $d_{sep} \leq 100$  kpc and an r-band magnitude difference of  $\Delta r (AB) \leq 1.5$  mag to approximate major  $\geq 4:1$  mass ratios under the assumption of a constant stellar mass-to-light ratio. We refine our selection by eliminating all pairs with actual stellar mass ratios  $M_1/M_2 > 4$ , where  $M_1$  is the stellar mass of the primary and most-massive galaxy in the pair. Mass ratios for the sample span the full range of primary galaxy mass, as shown in the left panel of Figure 3. The right panel of Figure 3 shows the stellar mass distribution for the mergers in light blue, and the total stellar mass for interactions in blue. This total stellar mass is a combination of the stellar mass for both the primary and companion galaxies.



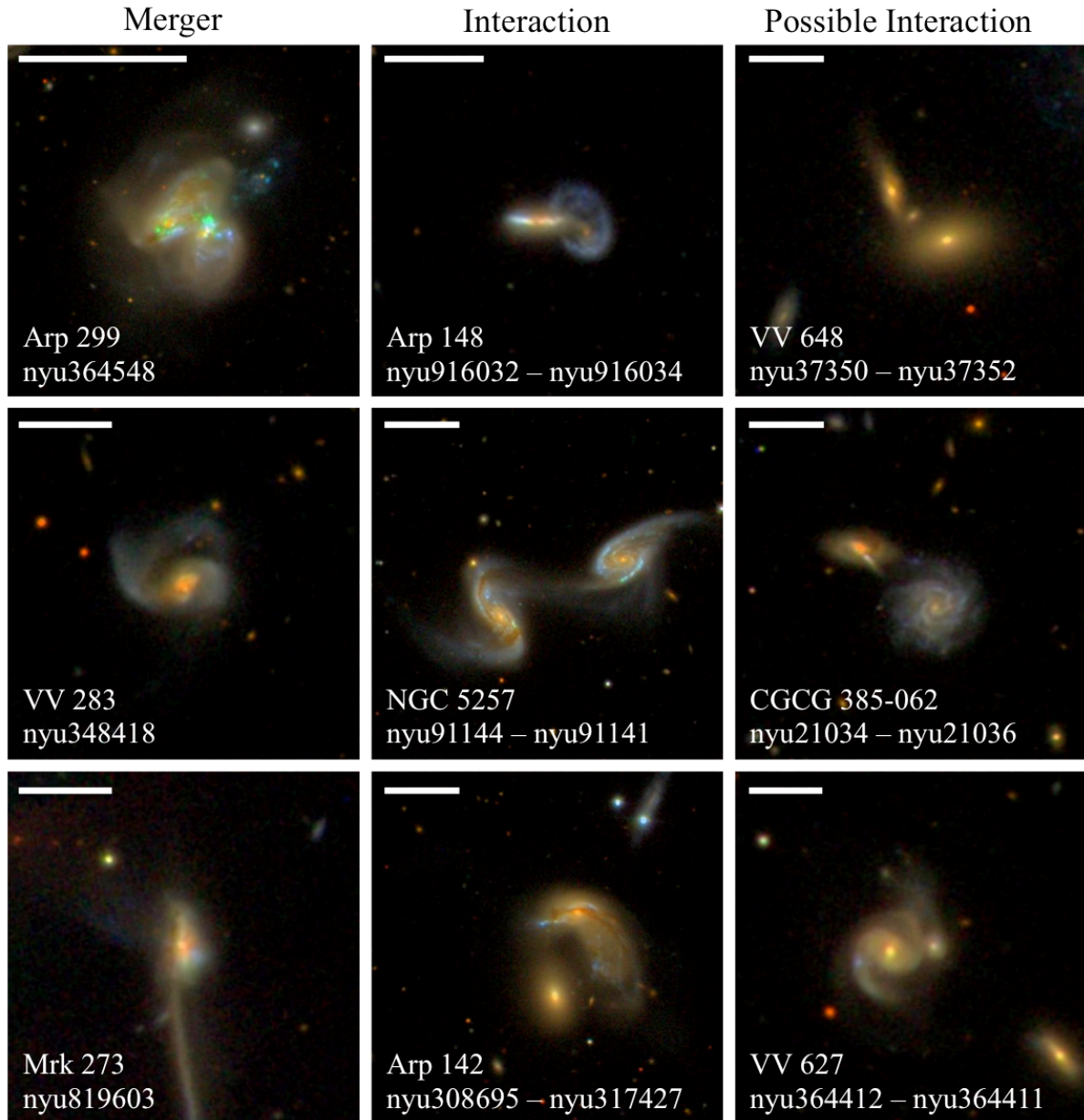


Figure 2. Example of Galaxies in the Merging and Interacting Sample  
*Notes.* Example of galaxies in this study. Sample subset is divided into ongoing mergers (left column), interactions (middle column), and possible interactions (right column). All images are cutouts of gri-combined color images downloaded from the SDSS Image List Tool. The white bar in the upper-left corner represents 20 kpc. Text in the bottom-left corner of each cutout is the proper name for the galaxy and the galaxy identification number for the galaxy or pair (from the DR4 NYU-VAGC; Blanton et al. 2005).

Table 1. Example from the Catalogue of Merging and Interacting Systems

nyu-ID	RA	DEC	Type	z	M <sub>star</sub>	Mass Ratio
(1)	(2)	(3)	(4)	(5)	(6)	(7)
nyu364548	172.13116	58.56437	m	0.010	10.4	---
nyu348418	195.45956	4.33338	m	0.037	10.8	---
nyu819603	206.17564	55.88717	m	0.037	10.8	---
nyu916032-nyu916034	165.97631	40.85003	i	0.035	10.6	3.9
nyu91144-nyu91141	204.99027	0.83082	i	0.023	11.1	1.2
nyu308695-nyu317427	144.43761	2.74738	i	0.023	11.2	1.1
nyu37350-nyu37352	39.71414	0.5087	i?	0.047	11.3	1.3
nyu21034-nyu21036	19.64195	-0.22837	i?	0.047	10.9	2.5
nyu364412-nyu364411	165.25207	57.78425	i?	0.048	11.3	2.6

*Notes.* Column (1): galaxy identification number (from the DR4 NYU-VAGC; Blanton et al. 2005). Columns (2) and (3): epoch J2000.0 equatorial coordinates in degrees from the SDSS. In the case of an interacting pair, the coordinates are that of the primary galaxy. Column (4): galaxy type based on visual classification given as follows: (m) merger, (i) interaction, (i?) possible interaction. Column (5): SDSS spectroscopic redshift from the NYU-VAGC.

Column (6): total stellar mass estimates in units of  $\log_{10} (M_{\odot})$  based on SDSS Petrosian photometry and Bell et al. (2003) M/L ratios. Column (7): mass ratio between the galaxies of the interacting or possibly interacting pairs.

The interacting population is split into two regimes: strongly interacting galaxies and possibly interacting galaxies (McIntosh et al. in prep). Strongly interacting galaxies are defined as pairs in which both galaxies appear visually disturbed or, in the case of a “mixed” interaction, that is a disk-spheroid interaction, the disk galaxy shows strong distortions that are interpreted to be caused by its nearest spheroidal neighbor (e.g., Arp 142 in Figure 2). Possibly interacting galaxies are defined by their pairings as follows: 1.) a spiral-spiral interaction showing weak tidal features in both galaxies or strong features in one, 2.) a spiral-elliptical interaction showing tidal features in the spiral galaxy, or 3.) an elliptical-elliptical interaction with an overlap between the nuclei and the outer stellar envelopes of both

galaxies. Our sample consists of 330 interactions with high classifier agreement (minimum of three out of four; one must be D.H.M.) and 795 possible interactions with lower agreement.

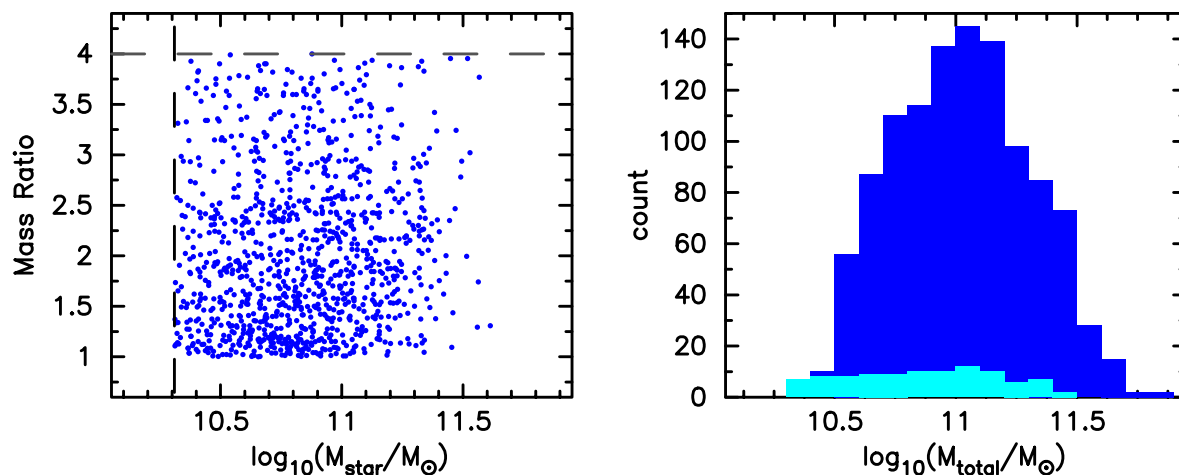


Figure 3. Mass Ratio and Stellar Mass for Merging and Interacting Sample

*Notes.* Left: For interactions, the mass ratio of the system versus the stellar mass of the primary (most massive) galaxy. The vertical dashed line at  $M_{\text{star}} = 2 \times 10^{10} M_{\odot}$  represents the mass cutoff for this sample. The horizontal dashed line at a mass ratio of 4.0 represents the mass ratio cutoff for a major interaction. Right: Stellar mass distribution for the full sample. Ongoing mergers are shown in light blue. The total mass of the interacting pair is given in blue.

## 2.2 SDSS Spectroscopic Emission Types

The SDSS fiber spectroscopy provides a reliable method of isolating different galaxy types through emission-line analysis. We collect all available SDSS DR7 spectroscopy for our sample and use the MPA-JHU emission-line analysis (Kauffmann et al. 2003, Brinchmann et al. 2004) to determine spectroscopic types where available. We use these spectroscopic types throughout our analysis.

The SDSS Main galaxy sample (Strauss et al. 2002) has an overall completeness of 92 percent for spectroscopy due to plate tiling to minimize fiber collisions (Blanton et al.

2003). To prevent collisions, fibers cannot be placed closer than 55 arcseconds from one another, limiting the number of spectroscopic targets per tile. For galaxy-galaxy interactions with small projected separations, this completeness drops significantly. For example, McIntosh et al. (2008) found that less than one-third of major interactions with a separation  $d_{\text{sep}} \leq 50 h^{-1} \text{ kpc}$  have spectroscopic information for both galaxies. For our sample, the spectroscopic completeness is 76 percent for ongoing mergers, 68 percent for primary interacting galaxies, and 47 percent for companion interacting galaxies. Of the interacting pairs, only 235 (21 percent) have SDSS spectroscopy for both galaxies, in agreement with McIntosh et al. (2008). Seventy percent of interacting pairs have SDSS spectroscopy for only one of the two galaxies. The remaining 106 interacting pairs have no SDSS spectroscopic information for either galaxy.

For the subset of our sample with spectra, spectroscopic emission types were determined through MPA-JHU emission line flux measurements from the SDSS fiber spectra (Kauffmann et al. 2003, Brinchmann et al. 2004). We use the spectroscopic emission types described in detail in McIntosh et al. (2014). Briefly, as shown in Figure 4, HII (pure star-forming), Composite (combination of SF and AGN), and AGN galaxies are determined using the criteria of Kauffmann et al. (2003) for galaxies with emission detected in the 4 lines of the standard BPT (Baldwin et al. 1981) diagram. LINER-type galaxies (Low Ionization Nuclear Emission Region galaxies) are separated from Seyferts using criteria from Schawinski et al. (2007). Spectroscopically quiescent (hereafter just quiescent) galaxies are defined as galaxies that lack detectable emission in all 4 BPT lines, that is non-star forming and inactive. For illustration, in Figure 5 we show examples of the SDSS spectra for galaxies classified as quiescent (top) and Seyfert (bottom). Blue and green circles highlight the

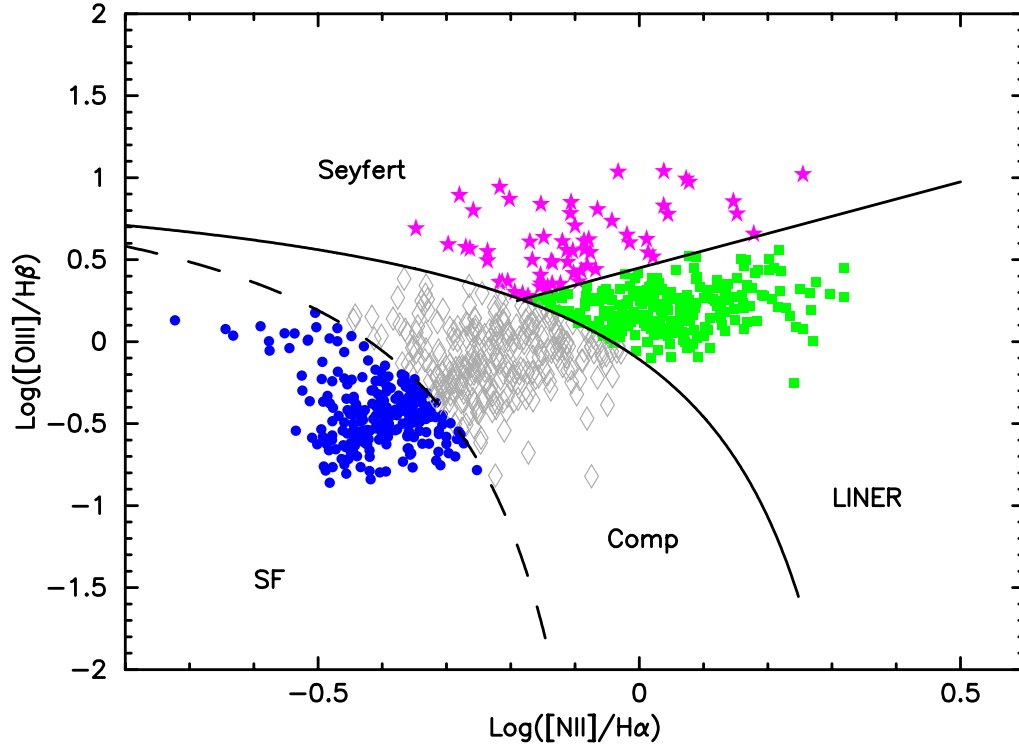


Figure 4. BPT Diagram for Merging and Interacting Galaxies

*Notes.* BPT Diagram (Baldwin et al. 1981) for the interacting and merging sample with sufficient spectroscopic data. Star forming galaxies are shown as blue circles, Composite galaxies as grey diamonds, LINER as green rectangles, and Seyfert galaxies as pink stars. The dashed curve between star forming and Composite galaxies (AGN activity) is from Kauffmann et al. (2003). The solid curve is from Kewley et al. (2001) and shows the theoretically derived division between Composite galaxies (some star formation) and true AGN. The additional line between the Seyfert and LINER populations is from Schawinski et al. (2007).

emission lines used in BPT analysis (see Figure 4). As shown, the quiescent galaxy lacks any detectable emission lines. In addition, we identify those galaxies with high  $[OIII] / H\alpha$  emission but insufficient lines for BPT analysis as weak emission-line galaxies using following Yan et al. (2006) and classify these as LINERS for our analysis; these galaxies make up 13 percent of the LINER population. Similarly, we classify weakly star-forming galaxies, that is galaxies with low  $[OIII] / H\alpha$  emissions, as part of the star forming (SF) or HII population for our analysis, which make up 12 percent of the SF population.

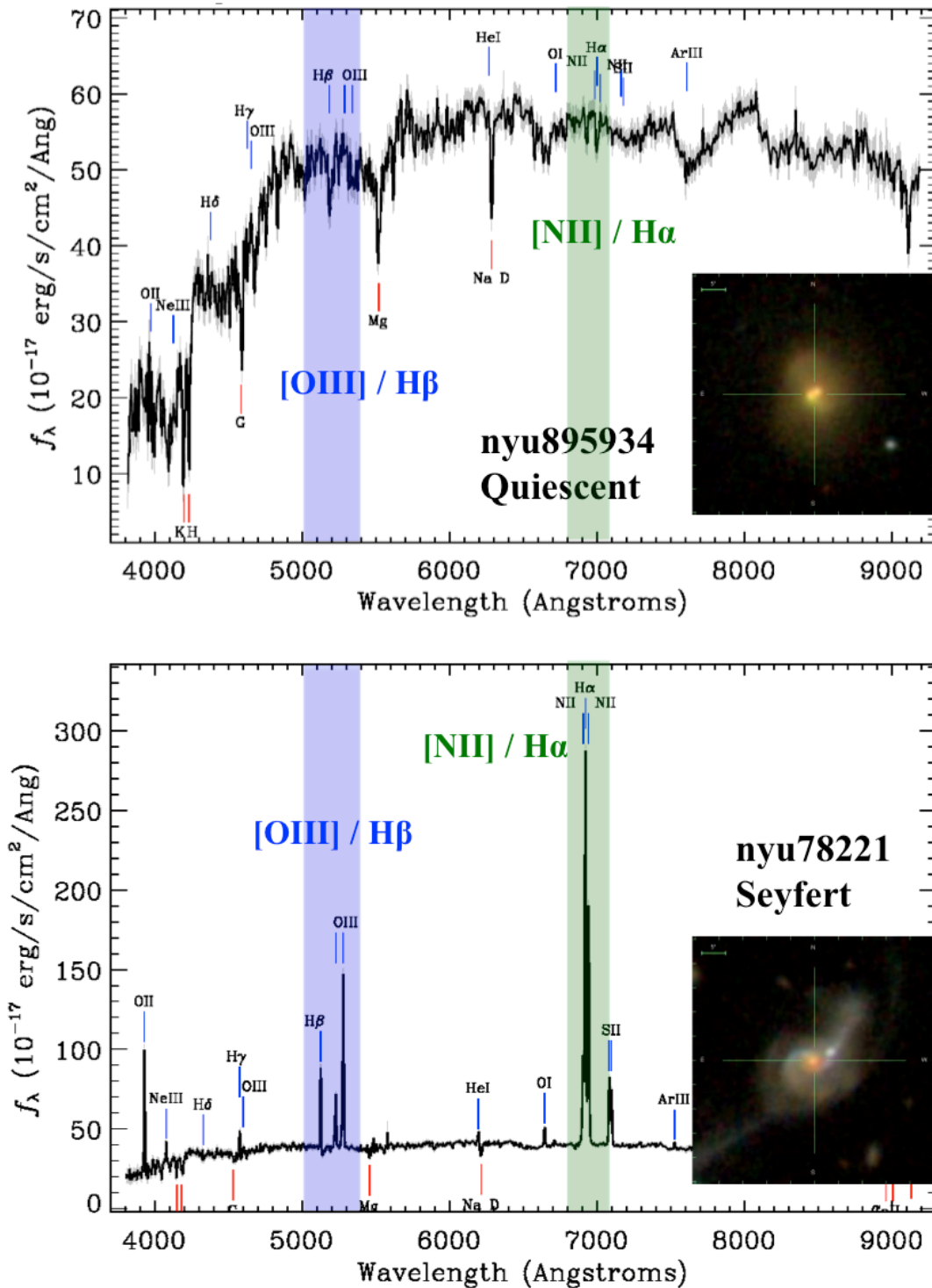


Figure 5. Example of SDSS Spectroscopy for Different Spectroscopic Types  
*Notes.* SDSS spectra for quiescent (top) and Seyfert (bottom) type galaxies from the merging sample. Identification numbers (from the DR4 NYU-VAGC; Blanton et al. 2005) and images from the SDSS Image List Tool are inset. The blue and green panels highlight the two emission lines used for each of the BPT Diagram (Baldwin et al. 1981) axes (Figure 4).

### 2.3 WISE Photometry

To identify dust-obscured AGNs, we use infrared colors from WISE observations. WISE is a 40-cm infrared space telescope funded by NASA and launched in December of 2009 (Wright et al. 2010). The WISE All-Sky Survey covered more than 99 percent of the sky with sensitivities more than 100 times better than the InfraRed Astronomical Satellite (IRAS) in the 12 micron band. We use data from the WISE All-Sky Source Catalog. This catalog contains positional and photometric information for over 563 million objects detected in the WISE images. We matched the sample from Chapter 2.1 to the WISE All-Sky catalog to obtain profile-fit magnitudes in four infrared channels: 3.4  $\mu\text{m}$  (W1), 4.6  $\mu\text{m}$  (W2), 12  $\mu\text{m}$  (W3), and 22  $\mu\text{m}$  (W4) (Wright et al. 2010). These bands have minimum  $5\sigma$  point source sensitivities of 0.008, 0.11, 0.8, and 6 mJy, respectively (Jarrett et al. 2011). The angular resolution of the first three bands (W1, W2, W3) is  $\sim 6$  arcseconds, while the 22 micron band (W4) has an angular resolution is  $\sim 12$  arcseconds. All WISE magnitudes are in the Vega system. WISE data can be accessed through the NASA/IPAC Infrared Science Archive (IRSA) pipeline and catalog information can be found in the WISE All-Sky Release Explanatory Supplement<sup>1</sup>.

We search the WISE All-Sky Source catalog for galaxy coordinate matches using a 15 arcseconds search radius centered on the SDSS coordinates. Many SDSS-WISE studies use a 3 arcseconds coordinate match (Shao et al. 2013, Yan et al. 2013, Donoso et al. 2012); Donoso et al. (2012) find that the overall SDSS-WISE false detection rate drops to 0.05 percent below the 3 arcseconds tolerance. However, we find that close projected pairs in our

---

<sup>1</sup> WISE data and documentation are available at <http://irsa.ipac.caltech.edu/Missions/wise.html>

interaction and possible interaction subsets require closer scrutiny. Because of the WISE 6 arcseconds resolution, it is necessary to check the coordinate matches of each interacting galaxy with a pair separation below that limit. We determine galaxy matches based on closest match to the SDSS coordinates provided by the master catalog. We check all galaxies with a

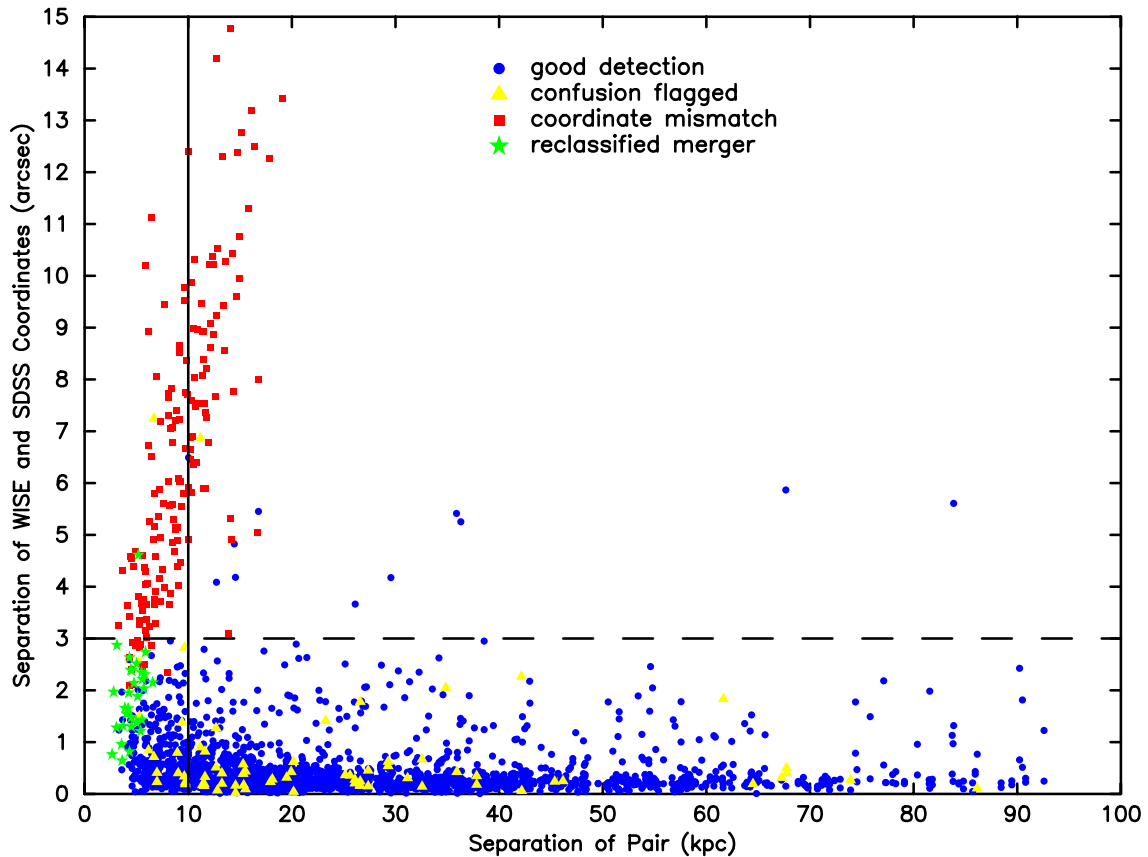


Figure 6. Separation of Coordinates vs. Separation of Pair for Interactions

*Notes.* Separation between the SDSS and the closest WISE detection coordinates for all pair galaxies versus separation between the primary and companion galaxies for interacting and possibly interacting galaxies. Blue circles represent galaxies with good WISE detections.

Yellow triangles show galaxies removed from the sample for contamination flagging. Galaxies removed from the sample for coordinate mismatches are shown as red squares (see Figure 7 and text for details). “Reclassified merger” galaxies are pair galaxies with both nuclei contained in a single 6 arcseconds WISE detection radius and are shown in the figure as green stars (see examples in Figure 8). Galaxies that fell below 10 arcseconds in pair separation (solid vertical line) or above 3 arcseconds in coordinate matching (dashed horizontal line) were checked in SDSS for correct location and flagged or removed from the sample as necessary.



pair separation of less than 10 arcseconds, marked by a vertical solid black line in the Figure 6, as well as all galaxies with a separation between the SDSS and WISE coordinates greater than 3 arcseconds, marked by the horizontal dashed black line in Figure 6. We eliminate several galaxies from the sample for having no WISE data, usually owing to a nearby object, like the companion galaxy, being detected instead, as shown by red squares in Figure 6. Examples of galaxies removed from the sample for this reason are shown in Figure 7. In most of these cases, the fainter companion, such as an early-type galaxy, is undetected by WISE. We note that only the pair galaxy undetected in WISE is removed from the sample; this leaves some interacting pairs with only one WISE detection. We reclassify 32 galaxy interactions as ongoing mergers, meaning that both galaxy nuclei fall within the 6 arcseconds radius of a single WISE detection (examples shown in Figure 8).

In addition to checking for accurate galaxy identifications, we cut any galaxies flagged as a spurious artifact (`cc_flags`) in the WISE catalog, as done in Stern et al. (2012). After this cut, the final interaction sample with WISE data consists of 307 interacting pairs and 762 possibly interacting pairs. Of these, 224 interactions and 645 possible interactions have WISE detections for both galaxies, 83 interactions have only one detection, and 117 possible interactions have only one detection. This gives a final sample of 1069 interacting pairs and 130 ongoing mergers (including the reclassified interactions). The WISE All-Sky Source catalog requires a S/N ratio of 5 in at least one band for any source included. We find that for our sample, all galaxies have a S/N ratio  $\geq 4$  in both the 3.4 and 4.6 micron bands, which are the critical bands for detecting obscured AGNs (Jarrett et al. 2011, Donoso et al. 2014, Assef et al. 2013). These cuts leave a final merger sample completeness of  $\sim 98$  percent. Our full interaction sample (interactions and possible interactions) completeness is

~ 89 percent, a significantly lower completeness than expected. The closeness of pairs in an interaction affects the completeness, as discussed above and seen in Figure 6 and 7.

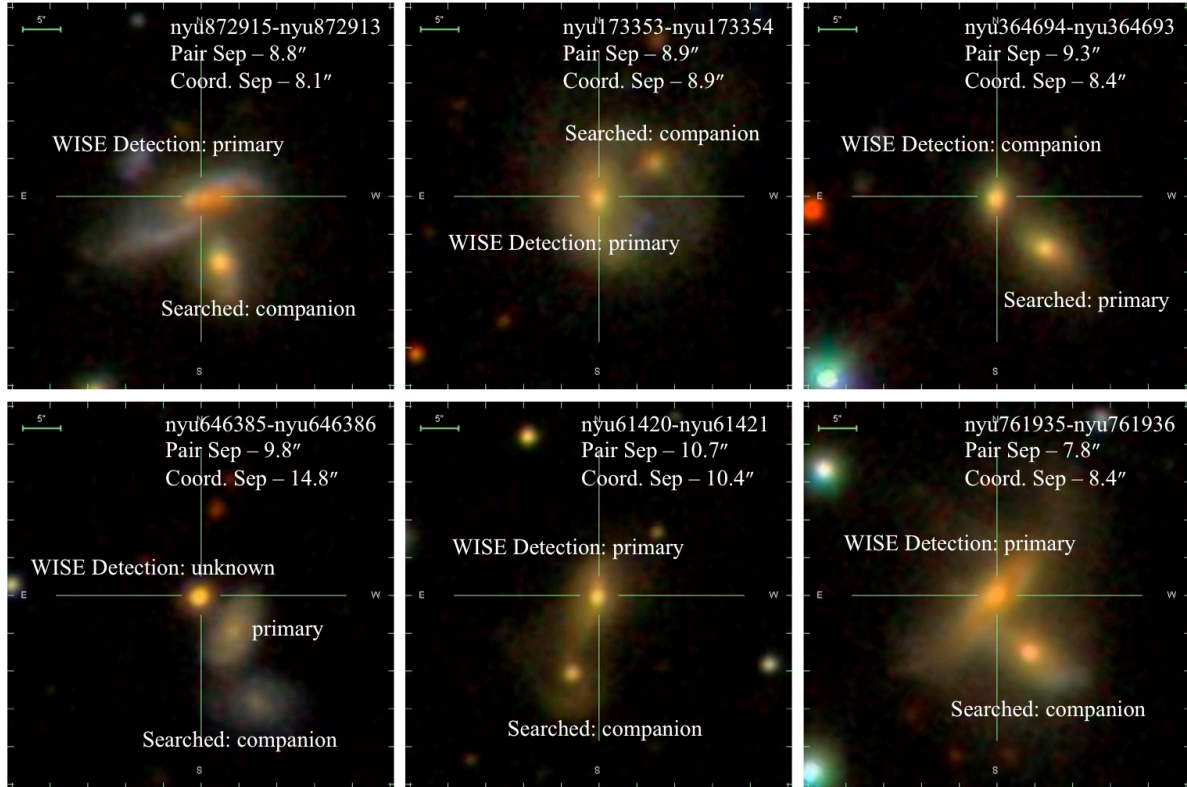


Figure 7. Example of Galaxies Removed from the WISE Sample

*Notes.* Examples of interaction galaxies removed from the sample because of a coordinate mismatch between SDSS and WISE. Pair identification numbers (from the DR4 NYU-VAGC; Blanton et al. 2005), angular separations, and coordinate separation between the SDSS and WISE are given in the upper-left corner of each image. All images are 51.2 x 51.2 arcsecond cutouts, centered on the WISE detection, from the SDSS Image List Tool.

“Searched” objects are the galaxies we attempt to acquire WISE data for and “WISE Detection” objects are the galaxy or object the WISE catalog matches as the closest object to the searched coordinates. In the case of nyu646385-nyu646386, we also label the primary galaxy.

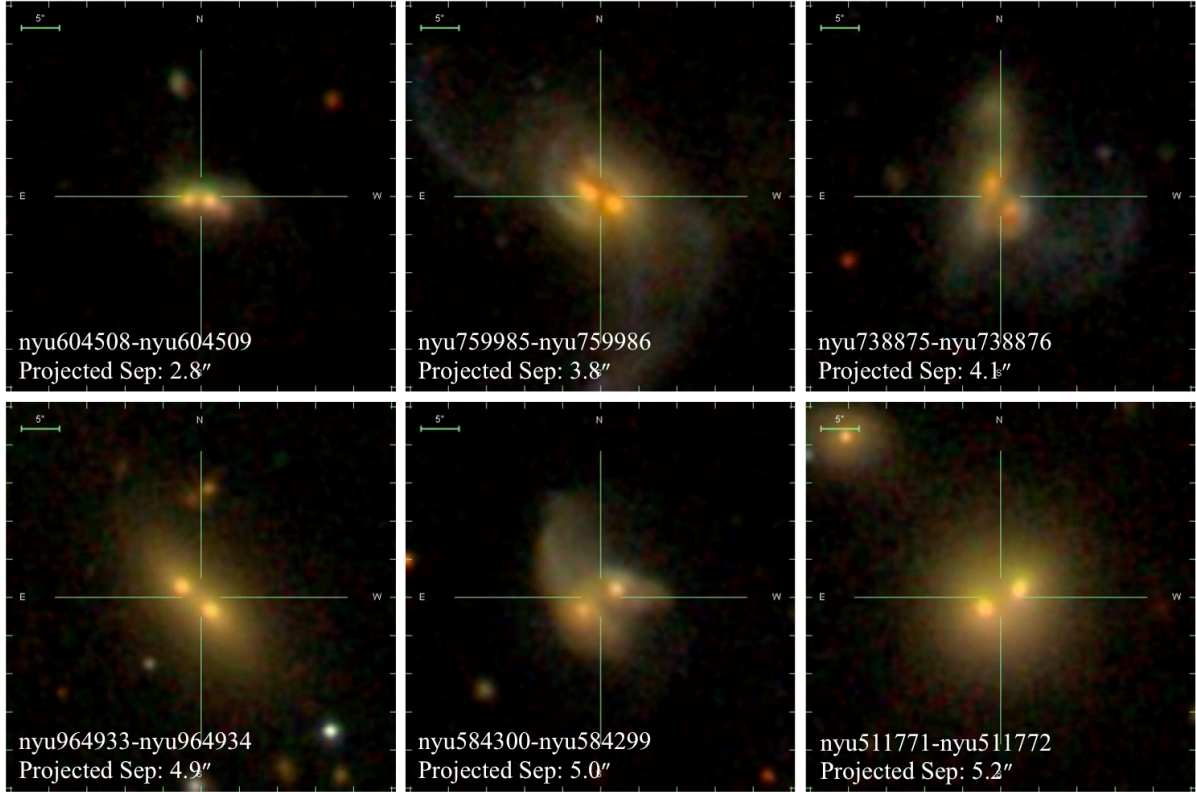


Figure 8. Example of Interactions Reclassified as Mergers for WISE Analysis

*Notes.* Example of galaxy-galaxy interactions reclassified as mergers for having a separation smaller than the angular resolution of WISE, or with a WISE detection centered between the two galaxies. All images are 51.2 x 51.2 arcsecond cutouts, centered on the WISE detection, from the SDSS Image List Tool. Pair identification numbers (from the DR4 NYU-VAGC; Blanton et al. 2005) and angular separations are given in the lower-left corner of each image.

## CHAPTER 3

### WISE COLOR ANALYSIS

To test for a connection between AGNs and merging or interacting galaxies, it is necessary to use a wavelength regime unaffected by dust attenuation in the center of these galaxies. Analysis of the WISE [3.4]-[4.6] vs. [4.6]-[12] color-color space has been shown to be an effective method of distinguishing galaxy and AGN activity among extended sources and separating high-redshift QSOs from stars among point sources (e.g., Wright et al. 2010, Yan 2013). In particular, this method is useful for isolating AGNs that escape optical detection due to dust obscuration in the nucleus (Jarrett et al. 2011, Mateos et al. 2012, Assef et al. 2013, Gürkan et al. 2014). In this chapter, we first use a control sample of 42,655 non-merging, non-interacting galaxies to map the WISE infrared color-color space of different spectroscopic types. We compare the location of these types to Wright et al. (2010). We then compare different methods of AGN selection. We apply the AGN selection criteria of Jarrett et al. (2011) to the control sample to find the occurrence of dusty AGNs (hereafter WISE AGNs) in our sample of non-merging, non-interacting galaxies. We also define our own AGN cut, an extension of the Jarrett et al. selection. Finally, we apply the Jarrett et al. (2011) WISE AGN cut to our merging and interacting sample. We compare the WISE AGN occurrence in merging and interacting galaxies to that of the control sample to highlight the connection between obscured AGN activity and merging and interacting galaxies.

#### **3.1 WISE Colors for Spectroscopic Types**

The WISE infrared color-color space has been theoretically mapped by galaxy classification based on simulated spectral energy distributions (Wright et al. 2010). Here, we

quantify the WISE color-color space for different galaxy spectroscopic types. We use a control sample of 42,655 non-interacting galaxies, from the SDSS DR4 with a WISE detection within a 3 arcsecond coordinate match, a S/N ratio  $\geq 4$  in both the 3.4 and 4.6 micron bands, and no spurious detection in the `cc_flag`, and adequate spectral information for spectroscopic type classification (see Chapter 2.1).

As shown in Figure 9, when the WISE [3.4]-[4.6] vs. [4.6]-[12] colors are plotted for different spectroscopic types, the majority of galaxies follow a roughly horizontal color-continuum in the [4.6]-[12] color from red and dead to star forming, with little change in the [3.4]-[4.6] color (Wright et al. 2010). Additionally, at redder [4.6]-[12] colors galaxies with increasing dust obscuration extend vertically into very red [3.4]-[4.6] colors (Wright et al. 2010, Jarrett et al. 2011). Conceptually, the [4.6]-[12] color is a measure of dust heating by star formation. We can expect quiescent, non-star forming galaxies, to have low [4.6]-[12] colors because they lack sufficient star formation. Similarly, we can expect star forming galaxies to have high [4.6]-[12] colors. The [3.4]-[4.6] color is representative of dust heating caused by an AGN. To illustrate this point, we show a galaxy spectral energy distribution (SED) in Figure 10. A galaxy is a combination of several components all emitting at their own wavelength, including older stars, new star formation, interstellar dust, and an AGN (Gruppioni et al. 2011). The SED of a galaxy is the combination of light from all the different components and can be combined with galaxy templates to show the estimated emission from each component of the galaxy. In Figure 10, the galaxy SED of IRAS 19254-7245 South (Nicastro et al. 1999) is shown with component templates overlaid. The WISE filters are shown as shaded regions as follows: 3.4 micron in blue, 4.6 micron in green, 12 micron in orange, and 22 micron in red. As shown in the 3.4 and 4.6 micron bands, the AGN

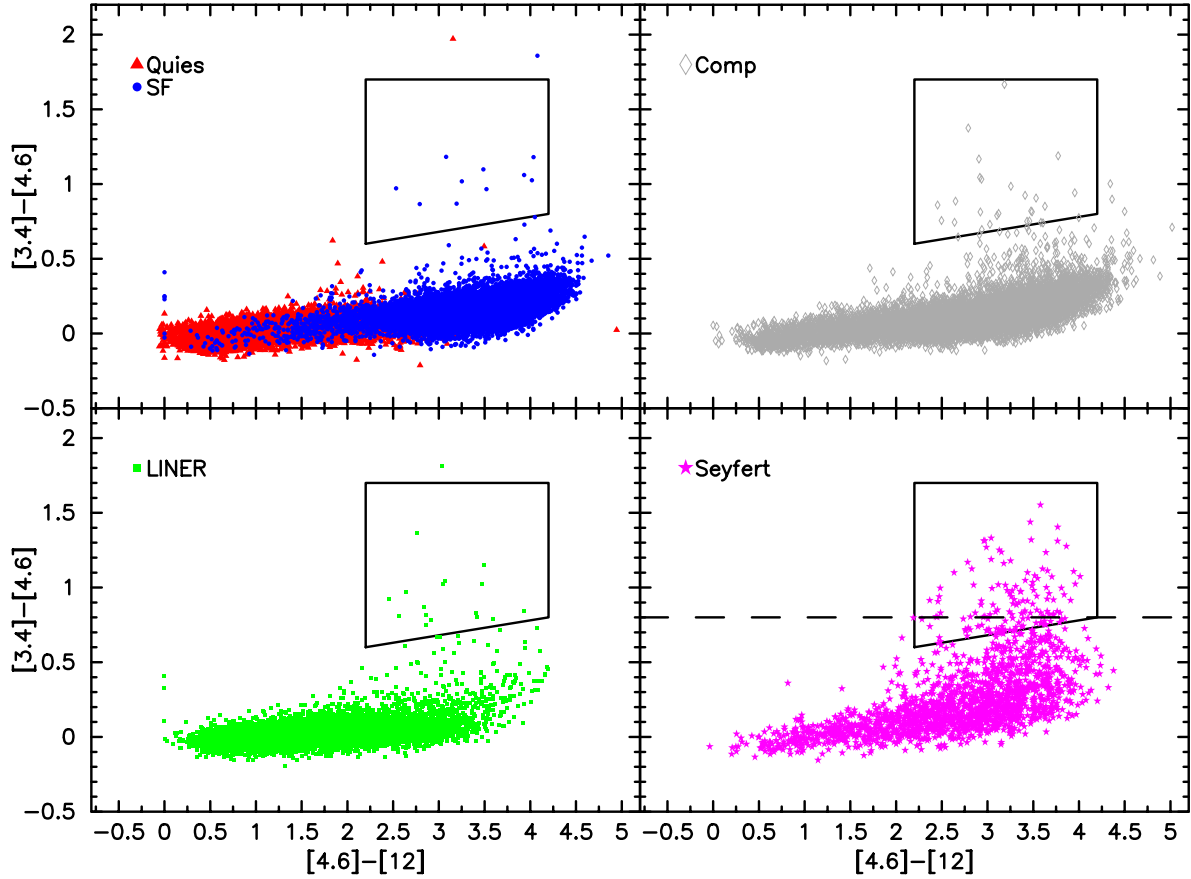


Figure 9. WISE Colors for Spectroscopic Types

*Notes.*  $[3.4]-[4.6]$  vs.  $[4.6]-[12]$  color plot for different galaxy spectroscopic types. In the upper-left, quiescent (red triangles) and star-forming (blue circles) galaxies are plotted together to show the bimodality of the infrared color-color space. In the upper-right and lower-left, composite (grey diamonds) and LINER (green squares) are shown to populate the full color-color continuum. In the bottom-right, Seyfert galaxies (pink stars) rise above the continuum into hot dusty color-color space. The box is defined as “WISE AGN” by Jarrett et al. (2011) and is populated only by heavily obscured AGN. The dashed line in the Seyfert panel at  $[3.4]-[4.6] \geq 0.8$  is used by Yan et al. (2013) to distinguish Type-2 AGN.

component (blue dashed-dotted line) of the galaxy shows a steep rise in the continuum, while all other galaxy components drop or remain constant across those pass bands. This increase in emission from the AGN component in the near infrared is what causes the red  $[3.4]-[4.6]$  colors. Thus galaxies with a  $[3.4]-[4.6]$  color close to zero have no AGN component, while

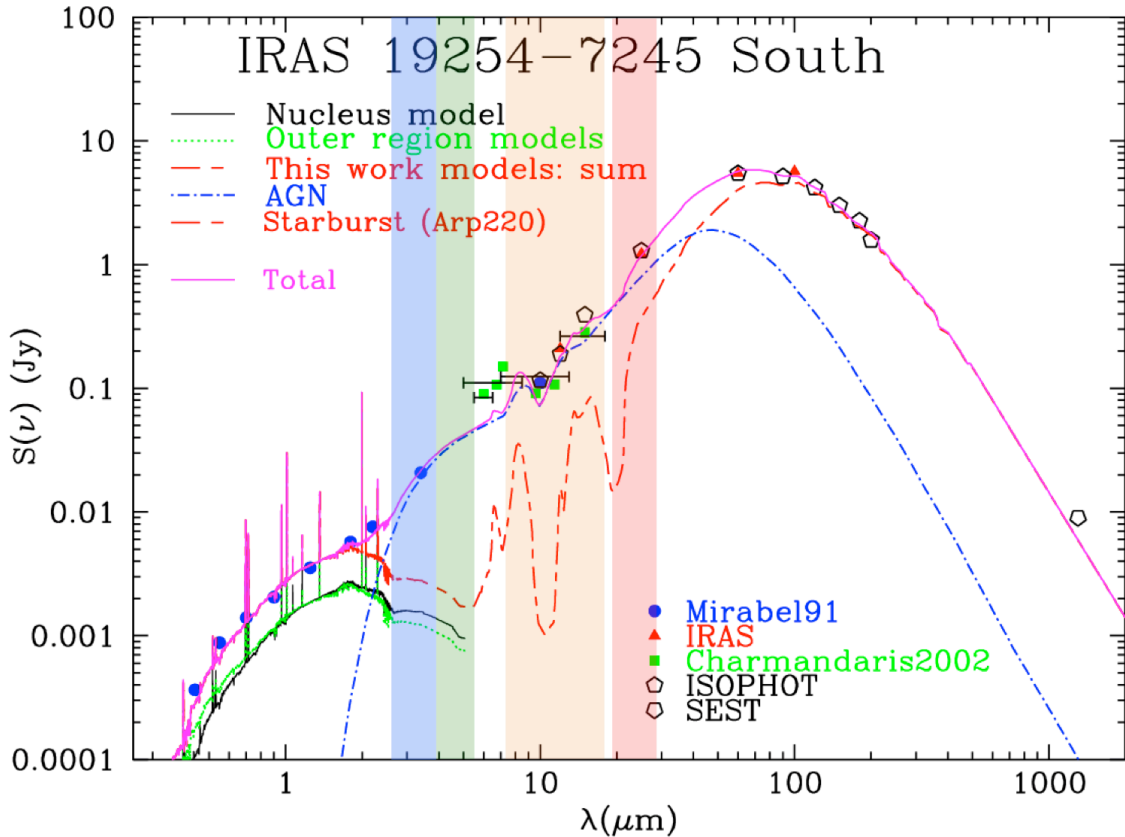


Figure 10. Galaxy Spectral Energy Distribution (SED)

*Source.* Nicastro et al. (1999)

*Notes.* The galaxy SED for IRAS 19254-7245 South (best fit shown in pink for data points from various studies; see Nicastro et al. 1999 for details) with model components; the SED gives the amount of energy received over a range of wavelengths. AGN component (from model) is shown as a blue dotted-dashed line. SED for Arp 220 (a starburst galaxy) is shown as a red dashed line. Black and green lines are from stellar emission. WISE filters are shown as shaded regions as follows: 3.4 micron (blue), 4.6 micron (green), 12 micron (orange), and 22 micron (red). The [3.4]-[4.6] color is the difference between the blue and green bands. As shown, the AGN model clearly increases in energy across those two bands, while other models drop off.

the population rising above the continuum are more likely to host a dust-enshrouded AGN.

This is shown in the Seyfert population of Figure 9.

In Figure 9, we show the WISE color-color space for the five spectroscopic types: quiescent and star forming, composite, LINER, and Seyfert. As shown in the upper-left plot,

the bluer color-color space is occupied mostly by quiescent galaxies (shown as red triangles) and star forming galaxies (shown as blue circles) are on the opposite, redder side of [4.6]-[12] color space. The majority of quiescent and star forming galaxies are separated by [4.6]-[12]  $\sim 2.25$ , as can be seen by their 80<sup>th</sup> percentile ranges in Table 2. Composite galaxies (grey diamonds), which are presumed to be a combination of SF and AGN, span nearly the full range of the continuum. LINER galaxies (green squares) span the continuum, though few are found redder than [4.6]-[12] = 3.5. Seyfert emission-line galaxies (shown as pink stars) span much of the continuum, yet a significant number of Seyfert galaxies fall above the general continuum at redder (hotter) [3.4]-[4.6] colors, inferring that a small fraction (less than one quarter) of Type 2 (obscured) Seyferts remain in the control population. Above [3.4]-[4.6]  $\geq 0.5$ , the population is dominated by Seyfert galaxies. This population of AGNs at redder [3.4]-[4.6] colors agrees well with the qualitative predictions of Wright et al. (2010).

Table 2. WISE Color Living Spaces of Spectroscopic Types

Type	N	[3.4] – [4.6]		[4.6] – [12]	
		Median	80%-tile Range	Median	80%-tile Range
(1)	(2)	(3)	(4)	(5)	(6)
Quies	9,416	0.02	-0.06 – 0.10	1.03	0.48 – 2.08
Composite	9,705	0.11	-0.01 – 0.26	2.90	1.51 – 3.73
SF	14,329	0.16	0.06 – 0.26	3.50	2.73 – 4.02
LINER	7,357	0.03	-0.06 – 0.12	1.72	0.81 – 2.76
Seyfert	1,848	0.18	0.00 – 0.61	2.80	1.35 – 3.62

*Notes.* Living spaces of spectroscopic types from analysis of [3.4]-[4.6] vs. [4.6]-[12] color-color plotting for a control sample of 42,655 non-interacting galaxies with stellar masses greater than  $2 \times 10^{10} M_{\odot}$  and redshifts  $0.01 \leq z \leq 0.08$ . Columns (1) and (2): the emission type and total number of that emission type in the control sample. Columns (3) and (4): the [3.4]-[4.6] color median value and 80<sup>th</sup> percentile range. Columns (5) and (6): the [4.6]-[12] color median value and 80<sup>th</sup> percentile range.



### 3.1.1 WISE AGN Selection

Several studies have shown that WISE color-color analysis is an effective method of isolating dusty AGNs from the general galaxy population (Jarrett et al. 2011, Yan et al. 2013, Satyapal et al. 2014). In the Seyfert panel of Figure 9, we highlight two AGN selection methods. First, the dashed line represents  $[3.4]-[4.6] \geq 0.8$ , a cut used by Yan et al. (2013), Assef et al. (2013), and Stern et al. (2012) to distinguish Type-2 AGNs from the general population. This straight cut also requires a WISE AGN to have  $[4.6] \geq 15.2$  to eliminate possible contamination by high-redshift elliptical and Sbc galaxies (Yan et al. 2013). We find that  $66^{+7}_{-8}$  percent of galaxies falling above this line are classified as Seyferts. Throughout this study, the errors on all numbers, fractions, and percentages are 95 percent binomial confidence intervals, unless otherwise stated. Second, the outlined box is defined using the criteria of Jarrett et al. (2011) to identify WISE AGN:

$$2.2 < [4.6] - [12] < 4.2 \quad (2)$$

$$0.1 \times [4.6] - [12] + 0.38 < [3.4] - [4.6] < 1.7 \quad (3).$$

As discussed in Jarrett et al. (2011), this box is chosen to enclose Seyfert galaxies and QSOs, while still lying above the star-forming galaxies at the blue end of the spectrum; fresh star formation can also cause a dust reddening effect. We find that  $73^{+6}_{-7}$  percent of galaxies falling in this box are classified as Seyfert galaxies. In Table 3, we show the results for each of these selection methods, broken down by spectroscopic types. We find similar results with both methods. We also include the WISE AGN selection method by Satyapal et al. (2014); a straight color cut of  $[3.4]-[4.6] \geq 0.5$ . We find that  $62^{+4}_{-5}$  percent of galaxies selected using this method are emission-selected Seyfert galaxies, making it a less robust, but still competitive, selection method.

Table 3. WISE AGN Fractions for Spectroscopic Subsample of High-Mass SDSS Galaxies

	WISE AGN	Ext. WISE AGN	[3.4]-[4.6] $\geq 0.8$	[3.4]-[4.6] $\geq 0.5$
Type	Jarrett et al.	This work	Yan et al.	Satyapal et al.
(1)	(2)	(3)	(4)	(5)
Quies	$0.00_{-0.00}^{+0.04}$ %	$0.02_{-0.02}^{+0.06}$ %	$0.01_{-0.01}^{+0.05}$ %	$0.03_{-0.02}^{+0.06}$ %
Composite	$0.26_{-0.08}^{+0.12}$ %	$1.30_{-0.21}^{+0.25}$ %	$0.21_{-0.07}^{+0.11}$ %	$0.97_{-0.18}^{+0.22}$ %
SF	$0.07_{-0.03}^{+0.06}$ %	$0.30_{-0.08}^{+0.10}$ %	$0.08_{-0.04}^{+0.06}$ %	$0.24_{-0.06}^{+0.10}$ %
LINER	$0.22_{-0.08}^{+0.14}$ %	$0.71_{-0.17}^{+0.22}$ %	$0.19_{-0.08}^{+0.13}$ %	$0.48_{-0.13}^{+0.19}$ %
Seyfert	$7.41_{-1.11}^{+1.29}$ %	$21.05_{-1.80}^{+1.92}$ %	$4.87_{-0.89}^{+1.08}$ %	$14.72_{-1.54}^{+1.69}$ %
Total	$0.44_{-0.06}^{+0.07}$ %	$1.44_{-0.11}^{+0.12}$ %	$0.32_{-0.05}^{+0.06}$ %	$1.03_{-0.91}^{+0.10}$ %

*Notes.* Fractions from analysis of [3.4]-[4.6] vs. [4.6]-[12] color-color plotting for a control sample of 42,655 non-interacting galaxies with stellar masses greater than  $2 \times 10^{10} M_{\odot}$  and redshifts  $0.01 \leq z \leq 0.08$ . Column (1): the galaxy emission type. Column (2): the percent of that emission type contained in the WISE AGN box defined by Jarrett et al. (2011). Column (3): the percent of that emission type contained in the Extended WISE AGN box defined in Chapter 3.1.2. Column (4): the percent of that emission type above the [3.4]-[4.6]  $\geq 0.8$  cut used by Yan et al. (2013). Column (5): the percent of that emission type above the [3.4]-[4.6]  $\geq 0.5$  cut used by Satyapal et al. (2014).

For this analysis, we choose the selection method defined by Jarrett et al. (2011). As shown in Figure 9 and discussed above, this selection is dominated by emission-line Seyfert galaxies, confirming the use of the Jarrett et al. (2011) box as a reliable method for isolating dusty AGNs. Indeed, the Seyfert population is the only spectroscopic type to have significant representation in the WISE AGN box. The majority of Seyferts fall outside this cut, and are presumably unobscured, Type 1 Seyferts. In addition, Composite galaxies, which are defined to be a combination of AGN and SF, make up around 13 percent of the Jarrett et al. box. The remainder of the WISE AGN population consists of LINER and HII galaxies (non-AGNs), which each make up around 14 percent of WISE AGNs. Because their WISE colors show clear dust signatures, we suggest that their optical classification may be unreliable and they

may be mislabeled AGNs. In addition to providing the color-color spaces of different emission types in WISE color space and testing the validity of multiple WISE AGN cuts, we also use our control population to examine the likelihood of a typical non-merging, non-interacting galaxy being classified as a WISE AGN. As shown in Table 3, the chance of a field galaxy being a WISE AGN is 0.38 - 0.51 percent. This result agrees well with the control analysis done by Satyapal et al. (2014).

### 3.1.2 Extended WISE AGN Selection

We also use the control population to define a lower, more liberal cutoff for the WISE AGN box used by Jarrett et al. (2011). This extension is used to include a population of galaxies that are presumably dustier than the normal continuum but still lie below the Jarrett et al. (2011) box, similar to the lower cut of  $[3.4]-[4.6] \geq 0.5$  used by Satyapal et al. (2014) and the Spitzer  $[3.6]-[4.5] \geq 0.5$  cut used by Ashby et al. (2009). In Figure 11, we show the WISE colors for all spectroscopic types from the control population. We see a noticeable fraction of Seyfert galaxies rising above the continuum, but not red enough at  $[3.4]-[4.6]$  to fall in Region A, as a WISE AGN. We define this new region, Region B, with Equation (2) from Chapter 3.1.1, and Equation (3) three-tenths of a magnitude below. We find that  $59^{+5}_{-5}$  percent of galaxies that fall in Region B are emission-line Seyfert galaxies. We combine Regions A and B into the Extended WISE AGN box. Of the galaxies contained in the Extended WISE AGN box,  $64^{+4}_{-4}$  percent are spectroscopically classified as Seyferts. The remaining population in the Extended WISE AGN box is made up mostly of Composite galaxies (~21 percent) and LINERs (~8 percent), both of which are considered possible or partial AGN systems. This high number of known AGNs and possible AGNs justifies this Extended WISE AGN cut as a plausible means of isolating dusty AGNs through WISE color-

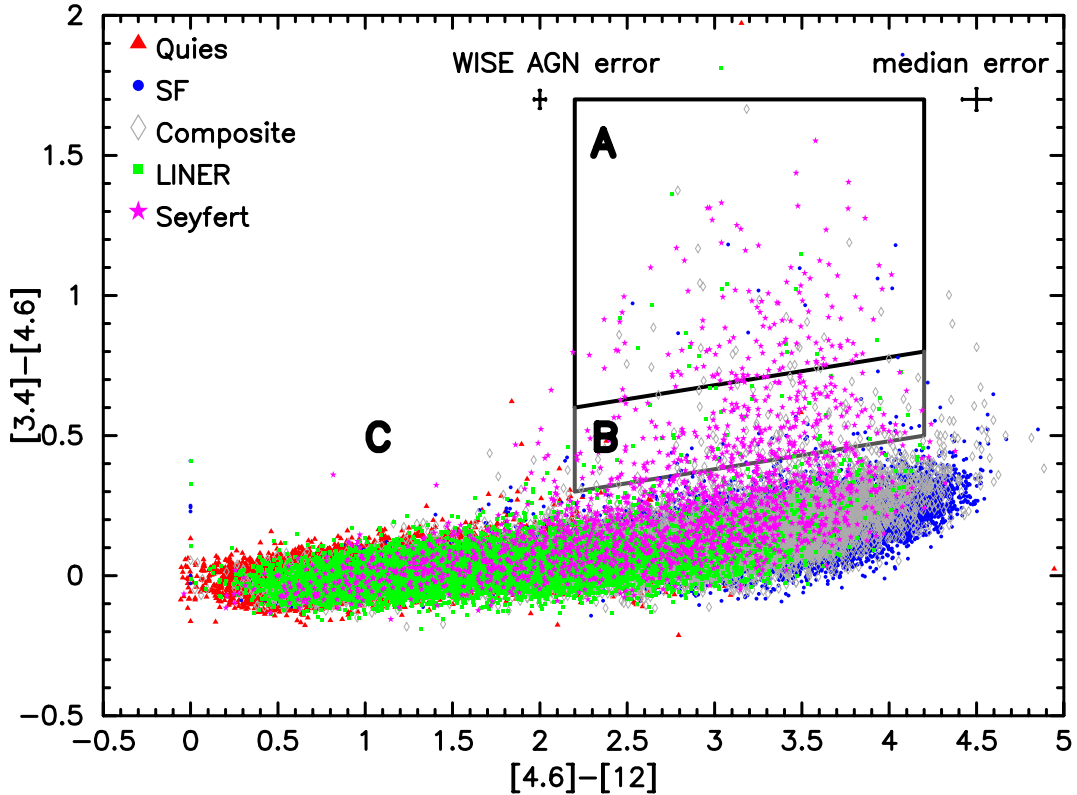


Figure 11. WISE Colors for 42,655 Control Galaxies

*Notes.*  $[3.4]-[4.6]$  vs.  $[4.6]-[12]$  plot for 42,655 control galaxies. Emission types are denoted as in Figure 9. The black box is defined as “WISE AGN” by Jarrett et al. (2011). The lower box represents the boundary of the Extended WISE AGN box (see text for details). The median color errors for the full control sample are given in the upper right-hand corner and the median color errors for the population of WISE AGN is given to the upper-left of the WISE AGN box. Regions for analysis of WISE AGN are noted as follows: (A) WISE AGN selected by Jarrett et al. (2011), (B) galaxies falling in the extended region, and (C) all galaxies not contained in regions A or B.

color analysis. In addition, we note that  $\sim 99$  percent of galaxies fall outside the Extended WISE AGN box. We do note that some galaxies are red enough in  $[3.4]-[4.6]$  to be associated with Extended WISE AGNs, but lie outside the  $[4.6]-[12]$  window. As explained in Jarrett et al. (2011), this small  $[4.6]-[12]$  window is chosen to leave out extreme starburst galaxies and dusty spiral galaxies. With this Extended WISE AGN cut, the likelihood of a

non-merging, non-interacting galaxy being a dusty AGN is 1.33 - 1.55 percent. Results for this Extended cut for different spectroscopic types are summarized in Table 3.

### 3.2 Incidence of Dusty AGNs in Mergers and Interactions

To compare the incidence of WISE AGNs among mergers and interactions to the frequency among non-interacting (control sample) galaxies, we analyze the WISE [3.4]-[4.6] and [4.6]-[12] colors of our sample of visually identified mergers and interactions in Figure 12. We include identifications without SDSS spectroscopic classification, shown as black x's. The majority of mergers and interactions follow the same general continuum of WISE colors as the control sample in Figure 9 and 11, with galaxies of each emission type populating similar areas in the continuum as the control population. Additionally, like the control sample a small fraction of galaxies fall above the continuum and a handful are found in the Jarrett et

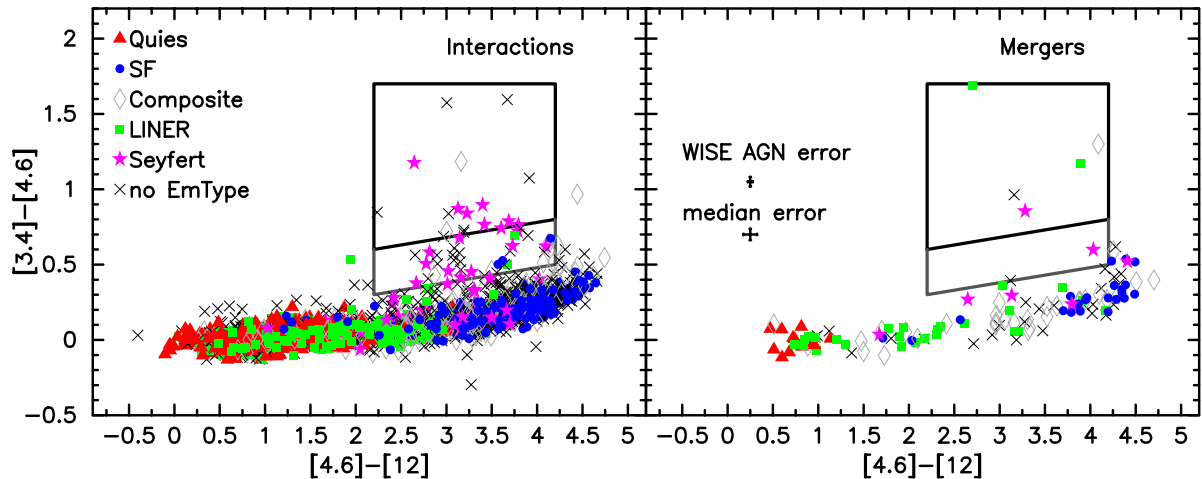


Figure 12. WISE Colors for Merging and Interacting Galaxies

*Notes.* [3.4]-[4.6] vs. [4.6]-[12] plot of interacting (left) and merging (right) galaxies. Spectroscopic types are denoted as in Figure 9 and shown in the left panel. Black x's represent mergers and interactions with no spectroscopic type. The black box is defined as "WISE AGN" by Jarrett et al. (2011). The lower box represents the boundary of the Extended WISE AGN box. The median color errors for the WISE AGN population and the full merging and interacting sample are given in the right panel.

al. (2011) WISE AGN box. Similar to the control sample, a larger fraction of Seyfert galaxies fall above the continuum than any other spectroscopic type. Of the Seyfert sample of 61 galaxies,  $15^{+11}_{-7}$  percent are defined as WISE AGNs from this analysis. This analysis also identifies 14 new WISE AGNs, 5 of which were previously classified as LINERs (2) or Composite galaxies (3), and 9 that previously had no spectroscopic classification.

Statistics for the analysis of the merging and interacting sample are shown in Table 4. Of the sample,  $5^{+6}_{-3}$  of the 130 mergers are classified as WISE AGNs ( $4^{+5}_{-2}$  percent). The interacting population has  $7^{+7}_{-4}$  galaxy pairs classified as WISE AGNs ( $2^{+3}_{-1}$  percent) and the possibly interacting population has  $10^{+8}_{-5}$  galaxy pairs classified as WISE AGNs ( $1.3^{+1.1}_{-0.6}$  percent), with one galaxy pair having both galaxies defined as WISE AGNs. When compared to our control sample (see Table 3), the merger population is 5 – 18 times more likely to be a dusty AGN than a non-merging field galaxy, and the overall interaction sample 2.6 – 4.9

Table 4. WISE AGN Fractions for Mergers and Interactions

Type	N	WISE AGN	Ext. WISE AGN	$[3.4]-[4.6] \geq 0.8$	$[3.4]-[4.6] \geq 0.5$
		Jarrett et al.	This work	Yan et al.	Satyapal et al.
(1)	(2)	(3)	(4)	(5)	(6)
m	130	$3.8^{+4.9}_{-2.1}$ %	$5.4^{+5.3}_{-2.8}$ %	$3.8^{+4.9}_{-2.1}$ %	$9.2^{+6.2}_{-3.9}$ %
i	307	$2.3^{+2.3}_{-1.2}$ %	$6.8^{+3.4}_{-2.3}$ %	$2.0^{+2.2}_{-1.1}$ %	$6.5^{+3.3}_{-2.2}$ %
i?	762	$1.3^{+1.1}_{-0.2}$ %	$4.3^{+1.7}_{-1.2}$ %	$0.7^{+0.8}_{-0.4}$ %	$3.9^{+1.7}_{-1.2}$ %

*Notes.* Fractions from analysis of  $[3.4]-[4.6]$  vs.  $[4.6]-[12]$  color-color plotting for the merging and interacting sample with stellar masses greater than  $2 \times 10^{10} M_{\odot}$  and redshifts  $0.01 \leq z \leq 0.08$ . Columns (1) and (2): the galaxy morphology type and number of sample galaxies of that type. Column (3): the percent of that morphology type contained in the WISE AGN box defined by Jarrett et al. (2011). Column (4): the percent of that morphology type contained in the Extended WISE AGN box defined in Chapter 3.1.2. Column (5): the percent of that morphology type above the  $[3.4]-[4.6] \geq 0.8$  cut used by Yan et al. (2013). Column (6): the percent of that morphology type above the  $[3.4]-[4.6] \geq 0.5$  cut used by Satyapal et al. (2014).

times more likely. When the Extended WISE AGN cut is used, we find that 3 – 11 percent of ongoing merger galaxies, 5 – 10 percent of interacting pairs, and 3 – 6 percent of possible interactions are classified as dusty AGNs. For this Extended cut, the merger sample is 2 – 6 times more likely to be a dusty AGN than a non-merging, non-interacting galaxy, and the overall interaction sample 2.9 – 4.2 times more likely.

## CHAPTER 4

### NATURE OF WISE AGN

The specific properties of WISE AGNs have been sparsely studied, particularly as they relate to a merger or interaction. To test whether merging and interacting WISE AGNs are unique, we compare their galaxy and pair properties to those of merging and interacting systems that are not WISE AGNs. For these comparisons, we use three subsamples of the merging and interacting population throughout this chapter: (i) WISE AGNs defined by the Jarrett et al. (2011) criteria and shown as region A in Figure 13, (ii) our more inclusive Extended WISE AGN selection of region A and presumably dusty systems in region B, and (iii) a control sample consisting of all merging and interacting galaxies not classified as Extended WISE AGNs, shown as region C and henceforth abbreviated as Region C. The galaxies in Region C lack any sign of warm dust heated by an AGN according to our WISE color analysis but do include a subset of emission-line Seyfert AGNs. In terms of properties, we will first analyze the relationship between WISE AGNs and galaxy or pair properties, including total stellar mass of mergers and interactions, mass ratio of interactions, and pair separation of interactions. We then examine the dependence of WISE AGNs on environmental properties (dark matter halo mass and central or satellite rank). We use the subsample of Seyfert galaxies in Region C to compare the accreting power of the WISE AGNs. Finally, we use SDSS ( $u - r$ ) and ( $r - z$ ) colors to find the likelihood of star formation in a WISE AGN merger or interaction. We note that all WISE magnitudes and color are in the Vega system, while SDSS colors are in AB. Additionally, we will treat interacting pairs as a single entity throughout this chapter.



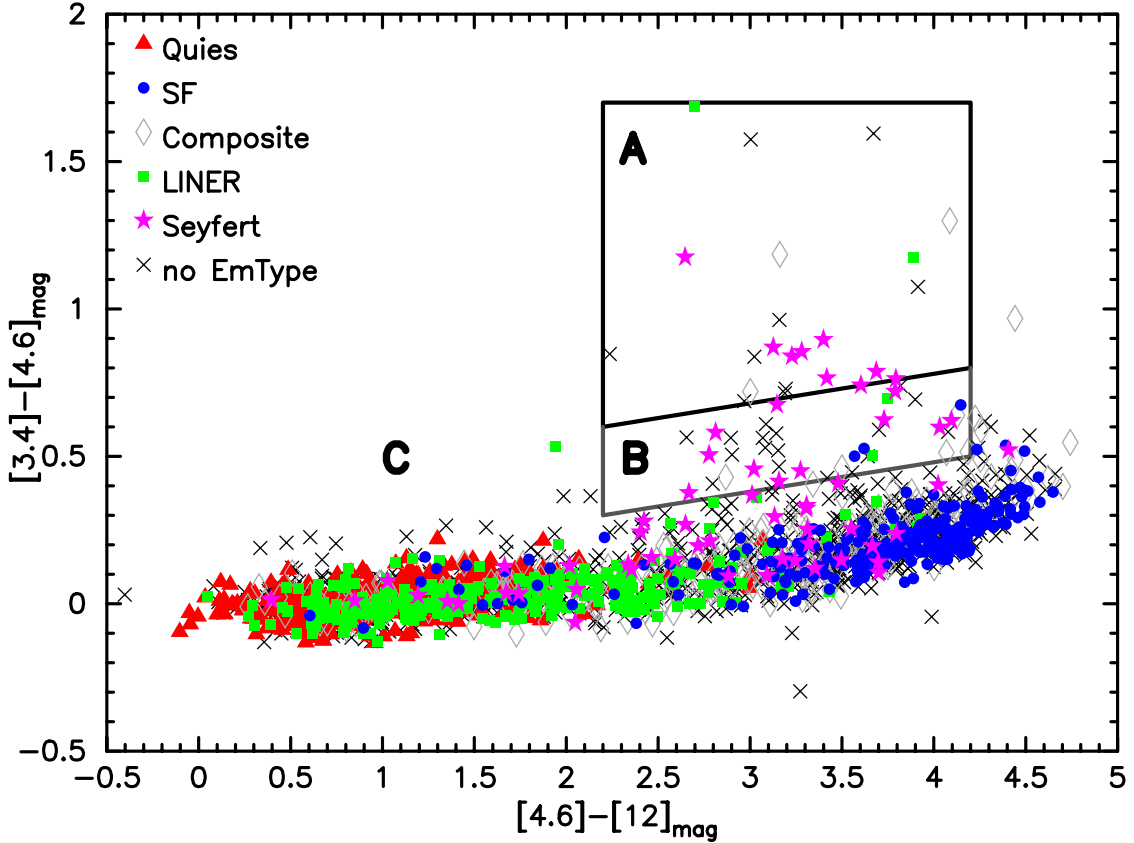


Figure 13. WISE Colors for Merging and Interacting Subsamples

*Notes.* Combined plot of  $[3.4]-[4.6]_{\text{mag}}$  vs.  $[4.6]-[12]_{\text{mag}}$  colors for merging and interacting galaxies.

Emission types are denoted as in Figure 12. Regions for analysis of WISE AGN properties are noted as follows: (A) WISE AGN selected by Jarrett et al. (2011), (B) galaxies falling in the extended region described in Chapter 3.1.2, and (C) all galaxies not contained in regions A or B.

#### 4.1 Galaxy and Pair Properties

The likelihood of finding an AGN in a merging or interacting system has been found to depend on a variety of properties, including mass ratios (Capelo et al. 2014, Ellison et al. 2011), pair separation (Ellison et al. 2011, Satyapal et al. 2014), and galaxy mass (Sabater et al. 2013). For our sample of high mass, low-redshift merging and interacting galaxies, we analyze the occurrence of WISE AGNs as a function of total stellar mass, mass ratio, and pair separation.

The correlation between AGNs and host galaxy mass has long been known. More than 80 percent of emission-line galaxies with  $M_{\text{star}} > 10^{11} M_{\odot}$  are classified as AGNs (Kauffmann et al. 2003). Occurrence of radio-loud AGNs rises with increasing host galaxy mass (Best et al. 2005). Sabater et al. (2013) found that galaxy mass has the strongest effect on the occurrence of AGNs, of any type. For our sample of mergers and interactions, the relative frequencies of total stellar mass (combined stellar mass of primary and companion in the case of interactions) are given in Figure 14 (left) for the three subpopulations described above as follows: WISE AGNs in dark blue, Extended WISE AGNs in hatched light blue, and Region C as a grey outline. While Region C does seem to span a wider range in masses, the WISE AGN populations may favor slightly lower stellar masses on average. To quantify this comparison, we make use of the two-sample Kolmogorov-Smirnov (K-S) test (Press et al. 1992): a test that returns a probability (p-value) of two separate distributions being

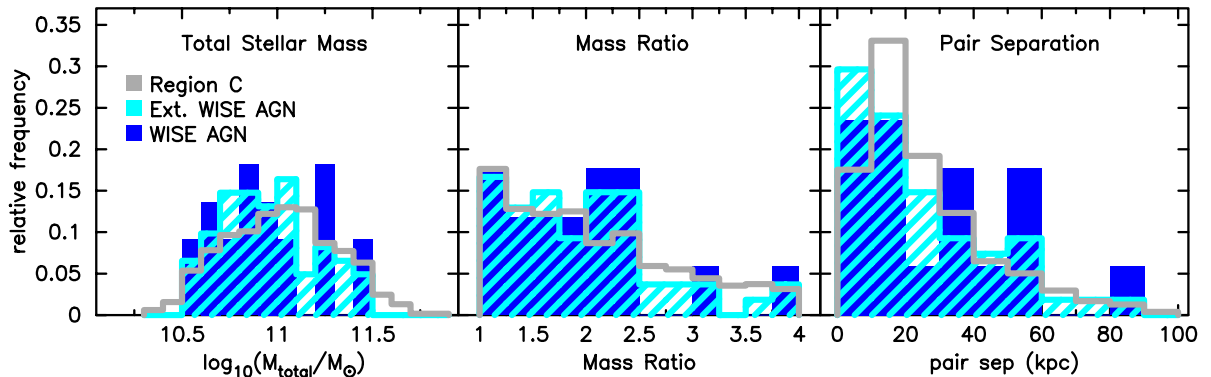


Figure 14. Distributions of Mass, Mass Ratio, and Pair Separation for Mergers and Interactions

*Notes.* Relative frequency distributions of interacting and merging galaxies for total stellar mass (left), mass ratio (middle), and proper pair separation in kpc (right). The subsample of merging and interacting galaxies not classified as Extended WISE AGNs is given in grey outline. For the right two plots, this control sample consists of interactions and possible interactions only (see Chapter 2 for details). WISE AGNs are given in dark blue and Extended WISE AGNs are given in light blue hatching.

statistically consistent with being drawn from the same of two separate distributions being statistically consistent with being drawn from the same parent distribution. In this study, the p-value is used to prove (to some significance) that the distribution of WISE AGNs/Ext. WISE AGNs is statistically different from other mergers and interactions in terms of a given property. For example, a significantly low p-value (less than 0.05) for a given property would suggest that the subset of WISE AGNs/Ext. WISE AGNs is statistically different from that of Region C, and thus the WISE AGN merging and interacting subset is unique from other mergers and interactions in terms of that property. The K-S test p-values for the distribution of stellar mass are shown in Table 5. The p-value for WISE AGNs is  $\sim 56$  percent and Extended WISE AGN population is  $\sim 9$  percent. Neither of these p-values are below the 2-sigma significance, and are thus consistent with the subset of WISE AGNs being drawn from

Table 5. K-S Test P-Values as a Proxy for Dusty AGN and Galaxy Property Relations

Galaxy Property	Region C Number	WISE AGN		Ext. WISE AGN	
		N	p-value	N	p-value
(1)	(2)	(3)	(4)	(5)	(6)
Stellar Mass	1,138	22	0.557	61	0.087
Mass Ratio	1,015	17	0.628	54	0.348
Pair Sep.	1,015	17	0.136	54	0.045
Halo Mass	1,137	22	0.141	60	0.017
Halo Mass (CEN)	888	18	0.093	48	0.018

*Notes.* K-S test p-values for the merging and interacting subsamples of WISE AGNs and Extended WISE AGNs. Column (1): the galaxy or pair property distribution tested. Column (2): the number of galaxies in the property distribution for Region C. Columns (3) and (4): the number of WISE AGN galaxies in the property distribution and the K-S test p-value for the WISE AGN population compared to Region C for that property. Columns (5) and (6): the number of Extended WISE AGN galaxies in the property distribution and the K-S test p-value for the Extended WISE AGN population compared to Region C for that property. We note that pair galaxies are treated as a single entity for this analysis.

the same stellar mass distribution as other mergers and interactions. However, the sharp drop in p-value for the larger sample of Extended WISE AGNs is suggestive of a unique distribution in stellar mass for the Extended subsample.

Simulations show that initial mass ratio between two galaxies in an interaction has a strong effect on black hole activity (Capelo et al. 2014) and star formation (Cox et al. 2008). Using hydrodynamic simulations, Capelo et al. (2014) found that a lower mass ratio (closer to equal mass) can produce a higher black hole accretion rate. Similarly, Cox et al. (2008) found in simulations that both the strength of a merger-driven starburst and the duration of the starburst can vary based on the mass ratio of the merger progenitors. The heightened activity in low-mass ratio interactions can be fundamentally described as the gravitational pull of the companion galaxy being large enough to tidally disrupt the primary galaxy, funneling gas to the center of both galaxies and igniting star formation and nuclear activity. In instances of high mass ratios (i.e. minor mergers), the companion galaxy is disrupted by the primary, but the companion is not gravitationally powerful enough to greatly affect the primary. Minor mergers can still produce heightened AGN activity, but a major merger will result in a higher accretion rate. Observationally, Ellison et al. (2011) performed a study of pair galaxies and found that the fraction of pairs identified as AGNs was greater for lower mass ratio pairs. The middle plot of Figure 14 shows the relative frequency distribution for the subsamples relative to mass ratio, as denoted in the total stellar mass plot. For all interaction subsets, there is a trend towards lower mass ratios. This is not surprising; interacting pairs are more likely to be visually classified if the two galaxies are of similar mass; closer mass galaxies will produce more tidal features making them easier to identify. The K-S p-value for this test, shown in Table 5, is above 60 percent for WISE AGNs and

around 35 percent for Extended WISE AGNs. These p-values and the distribution in Figure 14 related to the mass ratio of an interaction are consistent with the subsamples having the same distribution of mass ratios; thus, mass ratio does not appear to play a significant role in the occurrence of dusty AGNs in interacting galaxies.

Pair separation in an interacting pair of galaxies has been found to affect the occurrence of AGN in the pair (Ellison et al. 2011, Ellison et al. 2013, Satyapal et al. 2014). For a sample of close pairs, Ellison et al. (2011) found that the AGN fraction in pairs with a separation  $d_{\text{sep}} < 10 h_{70}^{-1} \text{kpc}$  is increased by a factor of  $\sim 2.5$  over non-interacting control galaxies. Satyapal et al. (2014) found that the infrared AGN fraction in a close pair increases with decreasing pair separation relative to the control, with post-merger galaxies having the highest likelihood of infrared AGN occurrence. In the right-hand plot of Figure 14, we show the relative frequency distributions in pair separation for the various subsamples. For all interaction subsets, there is a higher frequency at low pair separations ( $d_{\text{sep}} < 20 \text{kpc}$ ). The K-S test p-values (see Table 5) for this distribution are 14 percent for WISE AGNs and four percent for Extended WISE AGNs. While the p-value for WISE AGNs is not statistically low enough to suggest a difference in the pair separation distributions of dusty AGN interactions when compared to other interactions, the p-value for the Extended population is below 2-sigma (95% confidence), which suggests that pair separation is an important factor in the occurrence of dusty AGNs in interactions. Because the WISE AGN population is a subset of the Extended population, we speculate that a larger sample of WISE AGNs would provide a significant result. To test this hypothesis, we perform a K-S test on a pair of distinct, but overlapping Gaussian distributions with only 22 data points (matching the size of our WISE AGN sample, see the Appendix for details). We find that the p-value for these distributions

showed a significant difference only 50 percent of the time and was consistent with the two distributions being the same the rest of the time. This suggests that the small numbers in our WISE AGNs sample can reduce the significance of a given property.

## 4.2 Group Properties

The environment of an evolving galaxy system can have drastic effects on the properties of the galaxy. For example, virial shock heating within a galaxy's dark matter halo can heat the halo gas (Kereš et al. 2005, Dekel & Birnboim 2006), preventing it from collapsing to the center of the galaxy and accreting onto the black hole. We use the galaxy group catalog described in detail in Yang et al. (2007) to determine the relationship between dusty WISE AGNs and halo properties. This group catalog consists of environmental parameters for over 80,000 groups from the SDSS DR4 galaxy catalog, complete for bright sources ( $r(AB) \leq 18$  mag) at redshifts  $0.01 \leq z \leq 0.20$ . For this study, we use the following properties: (i) the galaxy rank within its halo based on highest stellar mass, with most massive ranked as central (CEN) and all less massive galaxies ranked as satellite (SAT); and (ii) a dark matter halo mass estimate based on group ranking and halo occupation statistics in the  $\Lambda$ CDM cosmological model. Briefly, groups were identified using a Friends of Friends algorithm (Davis et al. 1985). Next, a characteristic luminosity was determined for each group by combining the luminosities of the group members. This characteristic luminosity is used with an assumed mass-to-light ratio (M/L) to estimate a group halo mass with a corresponding halo size ( $r_{180}$ ) and velocity dispersion. Next, the selection of group members was revised by iterating the search window ( $\Delta r_{\text{proj}}$  and  $\Delta z$ ) defined by the halo, recalculating the characteristic luminosity and halo mass estimate, until convergence on a final selection of group members. The final characteristic luminosity of groups defined in this way was used to

construct an observed group luminosity function (LF). By matching the rank of an individual group in the LF to that of a dark matter halo drawn from a theoretical halo mass function assuming a  $\Lambda$ CDM cosmology, a robust estimate of the group's dark matter halo mass was determined. For galaxy groups with  $z \leq 0.08$ , the Yang et al. catalog is complete in halo mass for  $\log(M_{\text{halo}}/M_{\odot}) > 11.78$ . We note that two of our sample systems do not have group data in our catalog.

We examine the distribution of dark matter halo mass for WISE AGN mergers and interactions. In Figure 15, we show the relative frequency distribution of group halo mass for the following subsamples: Region C (left plot), WISE AGN mergers and interactions (middle plot), and Extended WISE AGN mergers and interactions (right plot). Based on the plot alone, we notice a higher fraction of WISE AGNs and Extended WISE AGNs are found in groups with dark matter halo masses  $\log(M_{\text{halo}}/M_{\odot}) < 13$ , thus they favor smaller mass haloes. We then use a K-S test to check for a difference in the distributions of dark matter halos for WISE AGN and Ext. WISE AGN mergers and interactions when compared to

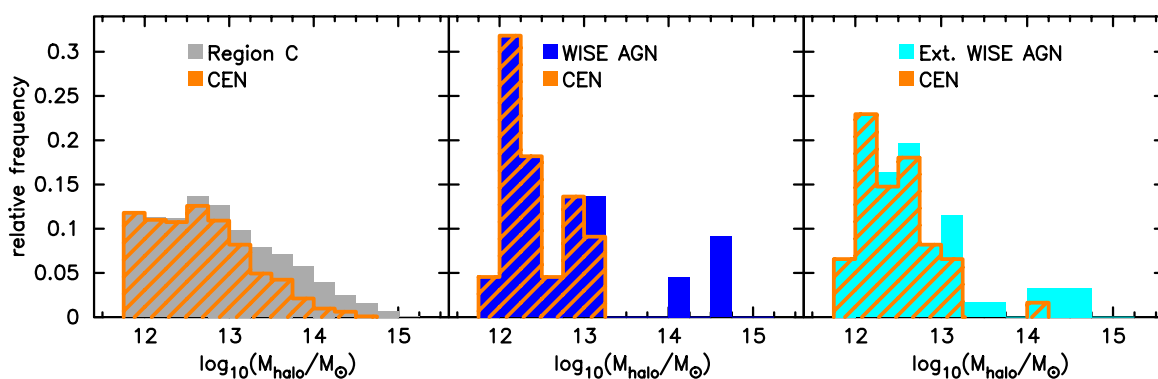


Figure 15. Distributions of Halo Mass for Mergers and Interactions

*Notes.* Relative frequency distribution of logarithmic halo mass for the following subsamples of merging and interacting galaxies: Region C (left, grey), WISE AGNs (middle, dark blue), and Extended WISE AGNs (right, light blue). For each plot, the orange-hatched regions represent the percent of that halo mass bin with centrally located galaxies.

Region C mergers and interactions. The p-values, shown in Table 5, are 14 percent and 1.7 percent for the WISE AGN and Extended WISE AGN subsets, respectively. The significantly low p-value for Extended WISE AGNs supports a relationship between the dark matter halo mass and the occurrence of dusty AGNs in mergers and interactions. Next, we look at the likelihood of a Region C merger or interaction to be defined as a CEN galaxy, meaning it is the most massive object in its halo. We find that  $\sim 78$  percent of this subsample is centrally located within their group. We find that  $\sim 81$  percent of WISE AGNs and  $\sim 80$  percent of Extended WISE AGNs are centrally located, suggesting that ranking relative to the group does not play a role in the occurrence of WISE AGNs.

By plotting the subset of CEN systems by dark matter halo mass (orange hatching in Figure 15), we find that mergers and interactions are less likely to be rank CEN at higher halo masses ( $\log (M_{\text{halo}}/M_{\odot}) > 13.25$ ). However, we notice that a higher fraction of Region C mergers and interactions are rank CEN at higher halo masses. This difference in CEN rank with halo mass motivates us to re-analyze our p-value for dark matter halo mass using centrally located mergers and interactions only. When we perform the K-S tests to compare dark matter halo mass of WISE AGNs and Extended WISE AGNs in central-identified mergers and interactions to dark matter halo mass of all other centrally located mergers and interactions, we find no significant deviation from the results presented in Table 5 (see Table 5 – Halo Mass (CEN)).

### **4.3 [OIII] Luminosity as an Indicator of AGN Power**

Galaxies classified as WISE AGNs have higher accretion rates, and are therefore more powerful, than non-WISE AGNs (Satyapal et al. 2014, Toba et al. 2014). To test the



distribution of AGN power in our sample of WISE AGNs, we use the [OIII]  $\lambda$ 5007 emission line strength. The [OIII]  $\lambda$ 5007 emission line is the strongest emission line in a typical Type-2 (obscured) AGN (Heckman et al. 2004), and can be used to indicate AGN luminosity. This line is less contaminated by star-formation than other optical emission lines (Kauffmann et al. 2003, Heckman et al. 2004). Previous works have already used this analysis to determine a correlation between WISE AGNs and AGN luminosity, or power. Toba et al. (2014) found that Type-2 AGNs also identified as WISE AGNs have typically larger  $L[\text{OIII}] / H\beta$  values than Type-2 AGNs not identified as WISE AGNs. Similarly, Satyapal et al. (2014) performed a study on close pairs of galaxies and found that a majority of the most powerful optical AGNs are also classified as WISE AGNs, though it should be noted that this population of optical AGNs also included LINERs, which are controversial and weak AGN at best.

To test if WISE AGNs are preferentially stronger than other AGNs, we use the subsample of emission-line Seyfert galaxies from Region C as a control population and compare their [OIII] luminosity to that of our WISE AGNs and Extended WISE AGNs. We calculate the [OIII] luminosity from the [OIII]  $\lambda$ 5007 flux provided in the spectroscopic catalog (see Chapter 2.2) using the flux-luminosity equation:

$$F = \frac{L}{4\pi d^2} \quad (4),$$

where  $F$  is the raw flux at a given wavelength in  $\text{ergs s}^{-1}\text{cm}^{-2}$ ,  $L$  is the luminosity of that wavelength in  $\text{ergs s}^{-1}$ , and  $d$  is the distance to the galaxy obtained from the redshift of the merger or pair in cm (Ryden 2003). The [OIII] luminosity distribution for the three subsamples of WISE AGNs (solid, blue), Extended WISE AGNs (light blue, hatched), and Region C Seyfert galaxies (pink, outline) are given in Figure 16. Red error bars are the 68

percent binomial confidence intervals for the Extended WISE AGN subset. The plot does show a tendency for Extended WISE AGNs to favor higher [OIII] luminosities, and therefore higher accretion rates. As done in Chapters 4.1 and 4.2, we use the K-S test p-value as a proxy for the relationship between WISE-selected AGNs and [OIII] luminosity by comparing the [OIII] luminosity of all WISE AGNs (including those already classified as Seyferts) to that of Region C AGNs (Seyferts). The K-S test result has a p-value of 0.12 for WISE AGNs and 0.016 for Extended WISE AGNs. The Extended WISE AGN p-value is significant enough to support a connection between merging and interacting WISE AGNs and AGN

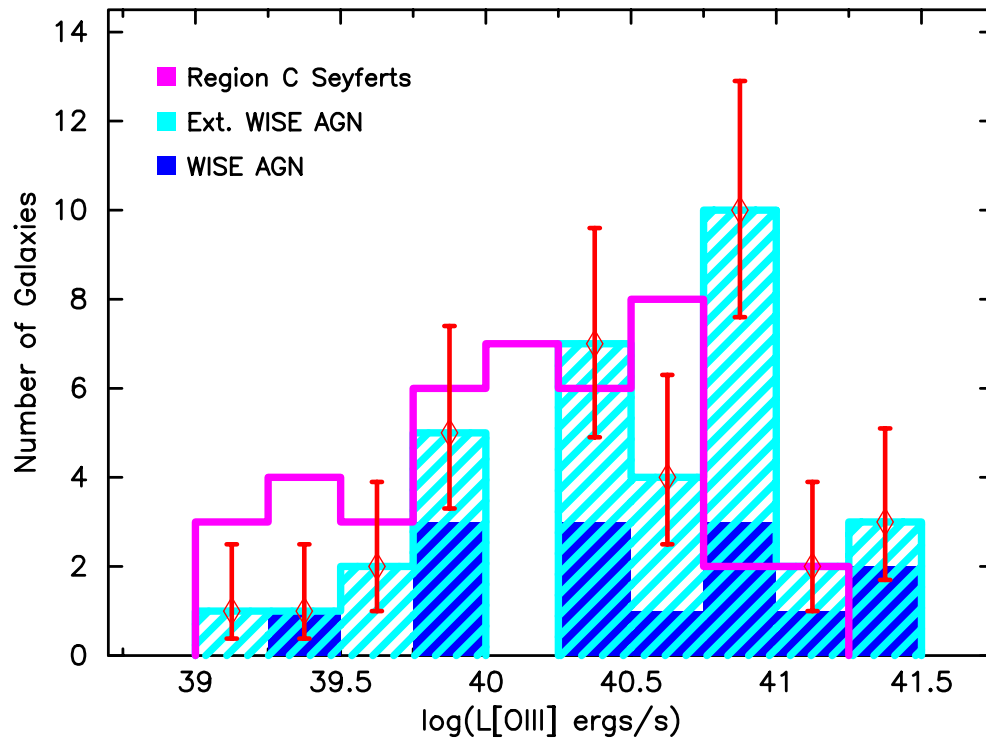


Figure 16. Distribution of [OIII] Luminosity for Merging and Interacting AGNs  
*Notes.* Property distribution of [OIII] luminosity for the following subsamples of merging and interacting galaxies: WISE AGNs (dark blue solid), Extended WISE AGNs (light blue hatching), and optically identified Seyfert galaxies from BPT analysis in Chapters 2.1 (pink outline). Red error bars are the 68 percent binomial confidence intervals for the Extended WISE AGN population.

power. While this result agrees with previous studies, we note that we may not find as strong of a trend in [OIII] luminosity as previous works due to the definition we use for optical AGNs. Our sample of optical AGNs only emission-line Seyfert galaxies for which the AGN identification is unambiguous. The inclusion of LINERs, as done in Satyapal et al. (2014), would shift the trend of the optical AGN to the lower power side, skewing the results to make WISE AGNs appear preferentially stronger.

#### **4.4 Star Formation of the Host Galaxy**

Bursts of new star formation have been undeniably linked to merging and interacting populations (Kennicutt et al. 1987, Barton et al. 2000, Lambas et al. 2003, Alonso et al. 2004, Ellison et al. 2008, Ellison et al. 2011). Kauffmann et al. (2003) showed that the most powerful AGNs have younger stellar populations than weak AGNs and normal galaxies, despite occurring in morphologically early-type galaxies. This strange mixture of young stars in a seemingly old system could imply a recent starburst, possibly a merger connection. To test for a correlation between WISE AGNs and star formation in the host galaxy, we use SDSS (u-r) vs. (r-z) colors to distinguish passive and star forming galaxies (Holden et al. 2012, McIntosh et al. 2014). These authors demonstrated that these colors effectively distinguish optically passive, red, non-star forming galaxies from dust-reddened star forming galaxies. We note that only the systems with spectroscopy are used in this analysis (see Chapter 2.2). The (u-r) and (r-z) colors are based on SDSS model magnitudes corrected for extinction and K-corrected to  $z = 0$ . In Figure 17, we show the SDSS (u-r) vs. (r-z) colors for the WISE AGN merging and interacting populations. The dark grey line from Holden et al. (2012) is the enclosure for galaxies identified as passive. For pair galaxies, we define a urz-SF pair as one in which one or both of the pair galaxies are urz-SF. An overwhelming

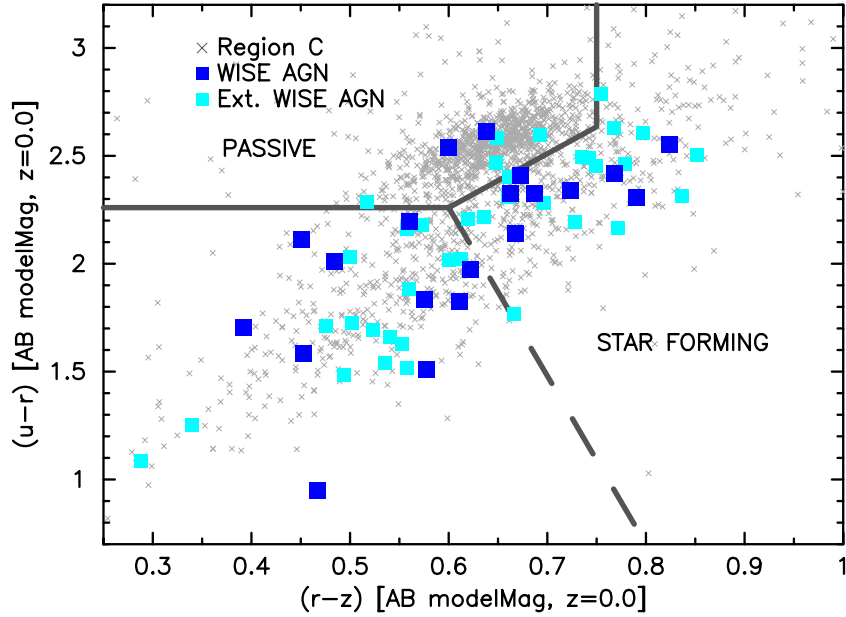


Figure 17. SDSS urz Color-Plot for Mergers and Interactions

*Notes.* SDSS (u-r) vs. (r-z) color plot for interacting and merging systems. Subsamples are denoted as follows: WISE AGNs are shown as dark blue squares, Extended WISE AGNs as light blue squares, and Region C as small grey x's. SDSS Model magnitudes are in the AB system and extinction- and K-corrected ( $z=0.0$ ), as done in McIntosh et al. (2014). The grey line by Holden et al. (2012) is the boundary between passive and star forming systems. The dashed grey line separates extremely blue galaxies (left) from normal star forming galaxies with dust (right).

majority of WISE AGNs lie in the star-forming region (70 – 97 percent). For the Extended population, this is 77 – 94 percent. This high level of star forming dusty AGNs implies a strong connection between AGN and star formation in merging and interacting galaxies. This result agrees with many other studies (Hickox et al. 2014, Kauffmann et al. 2003, Thacker et al. 2014).

In Figure 17, the dashed line is used to distinguish dusty star forming galaxies (right) from very blue, and thus unobscured, star forming galaxies. One interesting result of SDSS color-color analysis is the population of dusty AGN that are also very blue in the optical. Initially, this relationship seems contradictory. A WISE AGN-identified galaxy has a large

amount of dust in the nucleus, which should cause the galaxy to appear red in the optical wavelengths. A comparison of the galaxy morphologies reveals the key to this conundrum. In Figure 18, we show SDSS images of the 20 merging and interacting WISE AGNs with urz data. The interacting galaxies shown in the red outlines are the only “passive” systems identified in the urz analysis. Systems shown in the green outlines are urz-identified star forming galaxies that fall to the right (redder side) of the dashed line in Figure 17. Images contained in blue outlines are urz-selected star forming galaxies that would be considered unusually blue for a dusty galaxy, which is they fall to the left of the dashed line in Figure 17. While all of these WISE AGNs reside in galaxies with a disk component, the unusually blue galaxies have more distinct features of interaction, such as tidal tails and bridges, than their redder star forming counterparts. The urz-selected passive galaxies show little or no obvious signs of interaction. The difference in tidal features can explain why a dusty AGN galaxy could be blue in the optical. SDSS urz colors are representative of the entire galaxy; despite the dust-enshrouded core, a WISE AGN galaxy can still be blue in the optical colors if it has a star forming disk or tidal tails surrounding it.

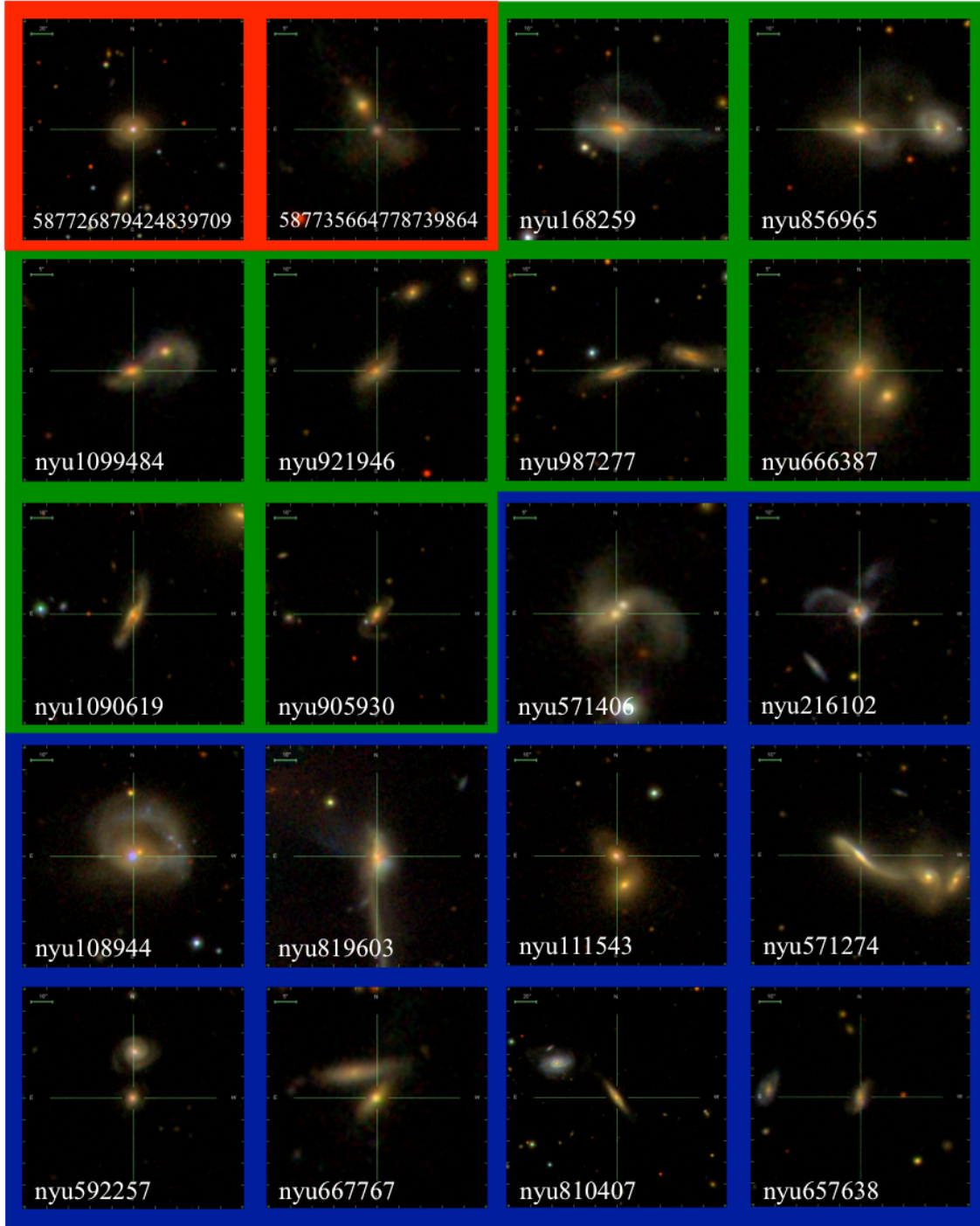


Figure 18. WISE AGN Mergers and Interactions

*Notes.* WISE AGN mergers and interactions used in SDSS color-color analysis, from the SDSS Image Tool. Sample subset is divided into urz-identified passive (red outlines) and star forming (blue and green outlines) systems. Galaxies with green outlines have redder (r-z) colors. Galaxies with blue outlines are redder in (r-z), but bluer in (u-r), and fall to the left of the dashed line in Figure 17. Galaxy identification numbers are given in the lower left corner of each thumbnail (from the DR4 NYU-VAGC; Blanton et al. 2005).

## CHAPTER 5

### DISCUSSION

The results we presented in Chapter 3 and 4 create several interesting questions about the merger process and the AGN-merger connection. In this chapter, we discuss some of these questions, including the likelihood of an AGN to be a merger or interaction, the likelihood of obscuration for a merging AGN, and the extent of contamination in the control population from misclassification. We also discuss the relation between dusty AGN mergers and star formation in the host galaxy. Finally, we discuss how our WISE AGN mergers and interactions differ from other mergers and interactions.

#### **5.1 The Dusty AGN-Merger Connection**

We find that merging galaxies (interactions) are 5 – 18 (1.0 – 2.5) times more likely to host a WISE AGN than a non-merging, non-interacting galaxy. Based on this higher likelihood of a merger to be a dusty AGN, we conclude that there is a link between dusty AGNs and merging systems. This dusty AGN-merger connection is consistent with the major merger model described by Hopkins et al. (2008) and others (Springel et al. 2005, DeBuhr et al. 2011, Volonteri et al. 2003), as well as many observational studies (Satyapal et al. 2014, Ellison et al. 2013, Nazaryan et al. 2014, Cotini et al. 2013, Karouzos et al. 2014). In particular, this result is in agreement with a similar study done by Satyapal et al. (2014), who found that mergers are 10 - 20 times more likely to host a dusty AGN than non-merging galaxies, and Ellison et al. (2013), who found that AGN occurrence in post-merger galaxies is 3.75 times higher than in close pairs. Additionally, this result could be consistent with the studies that found no AGN-merger connection, but were not working in a wavelength

compatible with severe dust attenuation (Villforth et al. 2014, Scott & Kaviraj 2014, Cisternas et al. 2011). For example, Scott & Kaviraj (2014) studied the incidence of BPT-selected AGN in merging galaxies and found no clear connection. This result suggests that many AGN in merging galaxies could be missed due to obscuration in the nucleus.

### 5.1.1 Obscured AGN Activity in Mergers

Studies done in the optical and X-ray may miss important AGN activity due to dust attenuation in the galaxy (Goulding et al. 2009, 2011). As predicted in major merger simulations (Hopkins et al. 2008, Springel et al. 2005, DeBuhr et al. 2011, Volonteri et al. 2003), the tidal forces in a merging pair can funnel gas to the nucleus for new star formation and AGN activity (Hann et al. 2009). The lack of a merger-AGN connection in optical and X-ray studies (Villforth et al. 2014, Scott et al. 2014, Cisternas et al. 2011) begs the question: how likely is a merging or interacting AGN to be obscured? To answer this, we compute the obscuration fraction:

$$\text{obscuration fraction} = \frac{N(\text{WISE AGN})}{N(\text{all AGN})} \quad (4),$$

where  $N(\text{WISE AGN})$  is the number of WISE AGN in a given population and  $N(\text{all AGN})$  is the combination of WISE AGNs and emission-line Seyfert galaxies. We also calculate the obscuration fraction based on the Extended WISE AGN population. Table 6 gives the obscuration fraction for merging, interacting, and possibly interacting galaxies, as well as the control sample described in Chapter 3.1. An AGN also classified as an ongoing merger is 2 – 6 times more likely to be obscured than an AGN control galaxy. For the interacting population, an AGN is 2 – 5 times more likely to be obscured than an AGN control galaxy. This likelihood drops in the possibly interacting population. This increase in nuclear activity



for more intense interacting stages is consistent with the major merger model (Hopkins et al. 2008, Springel et al. 2005, DeBuhr et al. 2011, Volonteri et al. 2003). In addition,  $\sim 50$  percent of merging AGNs are obscured, confirming as other studies have done (Stern et al. 2005, Gorjian et al. 2008) that the optical and X-ray wavelengths may not be adequate in selecting AGN mergers.

Table 6. Obscuration Fractions for Galaxy Morphologies

Type	WISE AGN	Extended WISE AGN
(1)	(2)	(3)
Mergers	$45^{+27}_{-24}$ %	$58^{+23}_{-26}$ %
Interactions	$39^{+20}_{-20}$ %	$75^{+12}_{-18}$ %
Possible Interactions	$23^{+14}_{-10}$ %	$55^{+12}_{-12}$ %
Control	$9.9^{+1.4}_{-1.3}$ %	$29.9^{+2.0}_{-1.9}$ %

*Notes.* Obscuration fraction for the following populations given in Column (1): merging galaxies, interacting pairs, possibly interacting pairs, and non-merging, non-interacting control galaxies. Column (2): obscuration fraction for the WISE AGN population using the criteria defined by Jarrett et al. (2011). Column (3): obscuration fraction for the Extended WISE AGN population using the criteria defined in Chapter 3.1.2.

### 5.1.2 Flipping the Coin: How Many AGN Are Mergers or Interactions?

Our results are consistent with a connection between merging and interacting systems and dust-obscured AGNs; however, this does not provide the whole picture of AGNs as they relate to merging galaxies. We test the connection between merging and interacting systems and all types of AGNs by combining our WISE AGNs/Extended WISE AGNs and emission-line Seyferts to find the fraction of the total AGN population that consists of a merger or interaction. In Table 7, we show the percentage of AGNs that are mergers or interactions for the following definitions of AGN: WISE AGNs (from Chapter 3), Extended WISE AGNs

(from Chapter 3), emission-line Seyferts, and a combination of WISE-selected AGNs and Seyferts (all AGNs). For illustration, we also show the percentage of mergers and interactions found outside the AGN populations. We find that the highest association between AGNs and mergers and interactions is for dusty, WISE-selected AGNs. There are 4 – 16 (2 – 5) times more mergers (interactions) in the WISE AGN population than in the non-AGN population. This higher fraction of mergers and interactions holds for the Extended WISE AGN population. However, the percentage of mergers and interactions found in the Seyfert population is similar to that found in the non-AGN population (and similarly for the combined WISE- and optically-selected populations). This strong connection to the dusty AGN population alone suggests that star formation (and therefore obscuration) in the nucleus of the system is the key to merger-induced AGN activity.

Table 7. Merging and Interacting Fractions in AGN Populations

AGN Population	N	Merging Galaxies	Interacting Pairs
(1)	(2)	(3)	(4)
WISE AGN	210	$2.83^{+3.07}_{-1.36}$ %	$8.10^{+4.48}_{-2.98}$ %
Ext. WISE AGN	673	$1.04^{+1.09}_{-0.54}$ %	$8.02^{+2.30}_{-1.82}$ %
Seyfert	1,909	$0.37^{+0.38}_{-0.19}$ %	$2.83^{+0.84}_{-0.66}$ %
WISE AGN and Seyfert	1,973	$0.56^{+0.44}_{-0.25}$ %	$3.19^{+0.87}_{-0.69}$ %
Ext. WISE AGN and Seyfert	2,171	$0.55^{+0.41}_{-0.31}$ %	$4.05^{+0.92}_{-0.75}$ %
Non-AGN	41,683	$0.28^{+0.06}_{-0.04}$ %	$2.35^{+0.15}_{-0.14}$ %

*Notes.* Fraction of merging and interacting systems for the following AGN populations given in Column (1): WISE AGN as defined by Jarrett et al. (2011), the Extended WISE AGN cut discussed in Chapter 3.1, emission-line Seyfert galaxies, the WISE AGN population combined with Seyfert galaxies, the Extended WISE AGN population combined with Seyfert galaxies, and all non-AGN systems. Column (2): the number (N) of galaxy systems contained in that population. Columns (3) and (4): the percent of an AGN population that consists of merging galaxies or interacting pairs, respectively.

### 5.1.3 Merger Contamination in the Control Sample

Motivated by the strong correlation between mergers and dusty AGNs relative to non-AGNs, we visually check all WISE AGNs in the control population of non-merging, non-interacting galaxies. We find that  $15 \pm 6$  percent of this population are visually disturbed or show signs of a recent or ongoing merger or interaction (major or minor), as classified by D. H. McIntosh and M. E. Weston. A sample of these galaxies is shown in Figure 19. The top six galaxies all show clear signs of a merger or interaction, including double nuclei and tidal features. The bottom six galaxies are all candidates for a minor merger or the post-merger phase. Galaxies nyu818795 and nyu8110 are elliptical galaxies with central dust lanes, suggesting recent star formation and possibly a minor merger. The remaining post-merger candidate galaxies are red in color, but show signs of star formation in their SDSS spectroscopy or, in the case of nyu560979, a clear blue ring of new star formation. This population of merging and interacting galaxies in the control sample suggests that the correlation between merging and interacting galaxies and dusty AGNs is stronger than our results indicate. We note that this sample of disturbed galaxies makes up less than 0.1 percent of our full control sample and should not drastically affect the results found in Chapter 3.1.

### 5.1.4 Physical Reasons for Only Some Mergers to be AGNs

Even with the addition of WISE AGN possible mergers and interactions from the control sample, only a small percentage of mergers and interactions are classified as WISE AGNs. This small fraction of AGN mergers motivates us to ask why all mergers don't appear to host an AGN. First, the simulations that predict AGNs in mergers (Hopkins et al. 2008, Springel et al. 2005, DeBuhr et al. 2011, Volonteri et al. 2003) require the presence of gas,

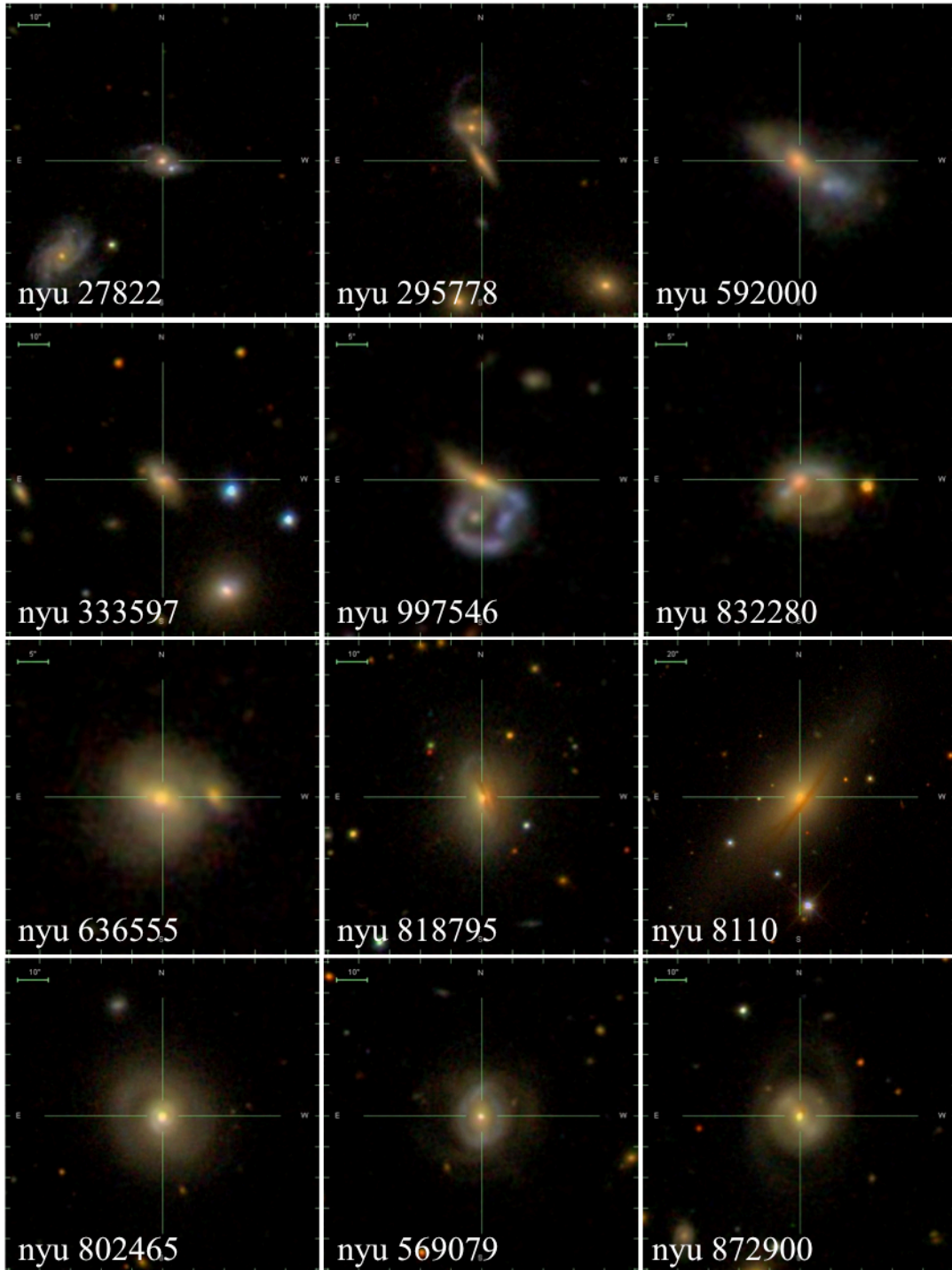


Figure 19. Examples of Misclassified Control Galaxies in the WISE AGN Population *Notes*. Sample of WISE AGN control galaxies (described in Chapter 3.1), from the SDSS Image Tool. The top six galaxies all show clear signs of a major merger or interaction, including double nuclei and tidal features. The bottom six galaxies are all candidates for a minor merger (nyu636555) or the post-merger phase. The galaxy identification numbers for the galaxies are provided (from the DR4 NYU-VAGC; Blanton et al. 2005).

which can be funneled into the nucleus of the system by the tidal forces. If the merger is dry (little to no gas), an AGN may not occur. Similarly, too much gas can swamp an AGN. For example, simulation work by Cox et al. (2008) showed that mergers with too much gas (higher than the critical gas density for star formation to begin) had a drop in starburst efficiency. Simulations by Cox et al. (2008) also revealed a burst efficiency dependence on the galaxy orbit, orientation, and progenitor disc structure. Observations and simulations (Haines et al. 2015, Cox et al. 2008) have shown that not all gas-rich mergers make a nuclear starburst (and therefore an AGN). Haines et al. (2015) found that  $\sim 75\%$  of merging galaxies show an enhancement in star formation over long timescales, but not a central starburst. Without a central concentration of gas for star formation, there will also be no gas accretion by an AGN. Possibly the most important reason that we do not find all mergers make AGN is the timing of the merger process. Because our sample is visually classified in a very broad-brush way, we don't know precisely where in the merger cycle our galaxies could be (coarsely,  $i$  = pre-merger,  $m$  = near coalescence) and it's very possible that our sample consists of many objects in the phases before, in between, or after AGN activity could be observed. As seen in the Major Merger model in Figure 1 (Hopkins et al. 2008), the window for AGN activity in the overall merger process is small. For our sample of merging galaxies, the system could be in any stage between Coalescence/(U)LIRG and Decay/K+A (phases  $d - g$ ). These phases combined consist of  $\sim 1 - 1.5$  Gyr, with the window of AGN activity making up about a quarter of that time. We therefore would expect a maximum  $\sim 25\%$  of our merging systems to be in the correct phase for AGN activity (assuming perfect gas content and mass ratio of progenitors). Lotz et al. (2010) found that the timescale for mergers detected through asymmetric features varies with gas content from 230 Myr – 1.4 Gyr, which

suggests that the timescale for observing the AGN phase of the merger could be even smaller than Hopkins et al. (2008) suggests.

## 5.2 Star Formation in Dusty AGN Mergers

The relationship between WISE AGN mergers and interactions and urz-selected star formers is not surprising. The major merger model by Hopkins et al. (2008) predicted that periods of high AGN activity should also achieve higher centrally concentrated star formation rates. The gas funneled to the center of the merger will both feed the AGN and collapse to form stars, which will in turn produce dust and obscure the AGN. Because of this relationship, one could argue that to get a true picture of the properties of WISE AGN mergers and interaction, one must compare only to other star forming galaxies. This idea is particularly intriguing for our sample, which contains a number of dry mergers and interactions that may not be truly interacting at all (see Chapter 2.1). When we cut our sample to only those mergers and interactions with urz-SF colors (for pairs, one of the two galaxies must be urz-SF), we find that the incidence of WISE AGN in mergers increases (3 – 14 percent). However, the incidence of WISE AGN mergers compared to the control sample remains constant (5 – 18 times). Statistics for this analysis are given in Table 8. We also perform all K-S tests in Chapter 4 for the population of urz-SF mergers and interactions only. We find that the majority of K-S test p-values rise for this round of tests, implying that star forming WISE AGN mergers and interactions are statistically equivalent to other star forming mergers and interactions. The p-values for mass ratio and pair separation drop, but not by a significant amount.

Table 8. WISE Color Analysis of Mergers and Interactions with urz-Selected Star Formation

Type	N	WISE AGN	Extended WISE AGN
(1)	(2)	(3)	(4)
Mergers	81	$6.2^{+7.5}_{-3.5}$ %	$8.6^{+8.1}_{-4.4}$ %
Interacting Pairs	725	$1.2^{+1.9}_{-0.1}$ %	$6.1^{+2.0}_{-1.5}$ %
Control	24,661	$0.7^{+0.1}_{-0.1}$ %	$2.1^{+0.2}_{-0.2}$ %

*Notes.* Fractions from analysis of [3.4]-[4.6] vs. [4.6]-[12] color-color plotting for the sample of urz-SF systems. Columns (1) and (2): the galaxy morphology type and number of galaxies of that type. Column (3): the percent of that morphology type contained in the WISE AGN box defined by Jarrett et al. (2011). Column (4): the percent of that morphology type contained in the Extended WISE AGN box defined in Chapter 3.1.2.

### 5.3 Properties of WISE AGN Mergers and Interactions

In Chapter 4, we examine multiple properties of merging and interacting systems to find any possible unique properties of WISE AGN mergers and interactions. We used 2-dimensional K-S tests to distinguish if subsets of dusty AGN mergers and interactions are statistically different from other mergers and interactions for a range of properties. We find that WISE AGN mergers and interactions favor smaller pair separations, smaller dark matter halo masses, and higher [OIII] luminosities (a proxy for AGN power) when compared to other mergers and interactions. Additionally, WISE AGN mergers and interactions show a strong relationship with urz-selected star forming galaxies (see Chapters 4.4 and 5.2).

#### 5.3.1 Pair Separations in Dusty AGN Mergers and Interactions

The relative frequency distribution of pair separations and the K-S test p-value for the pair separation of the Extended WISE AGN interactions (see Chapter 4.1) both support a preference of lower pair separations in dusty AGN interactions when compared to other interactions. This is consistent with studies that found an increasing number of AGN-

identified pairs with decreasing pair separation (Ellison et al. 2011, Ellison et al. 2013, Satyapal et al. 2014). Physically, it makes sense for dusty AGN systems to prefer lower separation because the torques in the interaction bring the gas and dust in the galaxy to the center of the interacting pair; a closer pair will therefore have more material in the nucleus to then accrete onto the black hole.

### 5.3.2 Dark Matter Halo Mass for Dusty AGN Mergers and Interactions

Both the relative frequency distribution of dark matter halo masses and the K-S test p-value for the dark matter halo mass of the Extended WISE AGN mergers and interactions (see Chapter 4.2) support a preference for lower dark matter halo masses in dusty AGN mergers and interactions when compared to other mergers and interactions. Physically, it makes sense for dusty AGN systems to favor lower halo masses. As shown in Chapter 4.2, the number of merging and interacting systems (of any subsample) drops sharply for halo masses greater than  $\sim 10^{14} M_{\odot}$  (similar to the masses of today's massive clusters). At these cluster masses, the dispersions are too high for mergers to occur frequently (Brodwin et al. 2013). Those mergers that do occur have little or no gas due to ram pressure stripping (McIntosh et al. 2014). Without the gas necessary for star formation and black hole accretion, we should also see a drop off in the occurrence of WISE AGNs at these masses. This is confirmed in Figure 15. Additionally, CEN ranked galaxies in halos with group masses less than  $\sim 10^{13} M_{\odot}$  have been found to continue forming stars at an efficient rate, despite being in a hot gas-dominated halo (Kereš et al. 2005). This confirms our results in Figure 15, in which the majority of dusty AGN mergers and interactions are centrally located in halos with masses less than  $10^{13} M_{\odot}$ .



### 5.3.3 The AGN Power in Dusty AGN Mergers and Interactions

In Chapter 4.3, we find that the [OIII] luminosity, a proxy for AGN power, is statistically higher for dusty AGN mergers and interactions in the Extended WISE AGN box. We find an inconclusive result when testing only the WISE AGNs, as selected using the criteria of Jarrett et al. (2011), but suggest this is due to the small numbers in that sample (see the Appendix). Physically, we would expect dusty AGNs in mergers and interactions to be stronger than Seyfert AGNs in mergers and interactions because a dusty AGN implies star formation in the nucleus of the system; therefore there is more accreting material surrounding the AGN. However, this implies that the WISE AGN subset, with its higher dust content, should be stronger on average than the Extended WISE AGN subset. This heightened [OIII] luminosity in the WISE AGN subsample, while not significant enough for the K-S test to reflect the difference, should be apparent in Figure 16. We suggest that the dust in the center of these mergers and interactions is causing extinction in the [OIII] line; the WISE AGN subset would have more dust and therefore more extinction. This physical interpretation implies that, without dust correction, the [OIII] line is underestimating the AGN power of infrared-selected dusty AGNs.

Despite dust extinction in the [OIII] line for our population of dusty AGN mergers and interactions, we still see a statistical difference in the distributions of [OIII] luminosity between the Extended WISE AGN and Region C mergers and interactions. Even without dust correction, the Extended population favors higher [OIII] luminosities. We further recognize that all K-S test values in Table 5 drop when we use the full Extended WISE AGN sample of mergers and interactions. This supports the idea that the larger dusty AGNs sample is making an already unique distribution clearer. To test this further, we perform the K-S

tests as done in Chapter 4 for only the galaxies in Region B (see Chapter 4) of the Extended population alone. We find that the majority of p-values rise for the Region B population when compared to the previous values for Extended WISE AGNs. This confirms that the larger sample size is likely the key reason that the p-values listed in Table 5 are consistently lower. However, the p-value for [OIII] luminosity for Region B drops to  $\sim 0.7$  percent, below the 1.6 percent for the full Extended region. This suggests that a large population of high-power AGNs live in the dusty region in between the Jarrett et al. box and the normal galaxy continuum. This further confirms our selection of this population as an additional set of AGNs and reflects the necessity to correct our [OIII] values for dust extinction so the true power of WISE AGN mergers and interactions can be recognized.

#### 5.3.4 Contamination of Region C by AGNs

The lack of a significant relationship between WISE AGNs and AGN power leads us to question if the Seyfert population (known AGNs) in Region C could be contaminating the results of our other K-S tests. To eliminate this possible contamination, we remove all emission-line Seyfert galaxies from Region C and perform K-S tests as done in Chapter 4. We find that all properties tested with the non-AGN Region C are similar to that of the previous tests shown in Table 5. We conclude that contamination of Region C by AGN does not affect to the WISE AGN merger and interaction properties. We conclude that the small sample size in the WISE AGN subsamples is the reason we see no distinct results for that population.

## CHAPTER 6

### SUMMARY

Encounters between gas-rich galaxies are predicted to drive gas to the centers of interacting and merging systems triggering new star formation and fueling an AGN (Hopkins et al. 2008, Springel et al. 2005, DeBuhr et al. 2011, Volonteri et al. 2003). Depending on the rate of SF, large amounts of obscuring dust (Clemens et al. 2013) can make detection of merger-induced activity difficult. We use data from WISE for a comprehensive study to find obscured AGNs in a sample of 1069 total interacting galaxies and 130 ongoing merger galaxies visually selected from SDSS DR4 with  $10^{10} M_{\odot}$  and  $0.01 < z < 0.08$ . Our results are summarized as follows:

- (i) We find an excess of obscured AGN activity in merging galaxies when compared to a control sample with the same redshift and mass constraints, indicating that merging systems are 5 – 18 times more likely to be an obscured AGN than a non-merging, non-interacting galaxy, at the 95 percent confidence level. This increase in obscured nuclear activity is consistent with the merger theory described in Hopkins et al. (2008) and others (Springel et al. 2005, DeBuhr et al. 2011, Volonteri et al. 2003).
- (ii) We define an Extended WISE AGN box to contain an additional set of unusually red (presumably dusty) galaxies. For this extended cut, the merger sample is 2 – 6 times more likely to be a dusty AGN than a non-merging, non-interacting galaxy.
- (iii) To test for unique properties of dusty AGN mergers and interactions, we analyze a set of key properties of WISE AGN mergers and interactions. We find that dusty AGN mergers

and interactions favor smaller pair separations, smaller dark matter halo masses, and higher [OIII] luminosities (a proxy for AGN power) than other mergers and interactions.

(iv) We find that all dusty AGN mergers and nearly all dusty AGN interactions are found in star-forming galaxies. Those dusty AGN interactions not classified as star forming show little signs of interaction and may be non-interacting interlopers from classifier error. This connection between obscured nuclear activity and star formation is consistent with the merger theory described in Hopkins et al. (2008) and others (Springel et al. 2005, DeBuhr et al. 2011, Volonteri et al. 2003).

(v) We find that AGNs also classified as ongoing mergers are 2 – 6 times more likely to be obscured than AGNs in non-merging, non-interacting galaxies. Around half of merging AGNs are obscured, suggesting that shorter wavelengths will be inadequate in selecting AGNs in merging systems. We find no association between merging systems and optically identified AGNs (Seyferts), suggesting that central star formation (and thus dust obscuration) is the key to making an AGN in a merger.

We conclude that the major merger model simulations (Hopkins et al. 2008, Springel et al. 2005, DeBuhr et al. 2011, Volonteri et al. 2003) have been empirically verified to be correct. Gas-rich major mergers cause bursts of star formation and fuel AGNs. The star formation produces dust, which obscures the AGN and reradiates in the thermal infrared. Because of this obscuration, optical and X-ray surveys necessarily see not only an incomplete picture, but are also biased against measuring the true merger rate, star formation rate, AGN rate, and demographics. Nothing in our study supports the Dekel picture (Zolotov et al. 2014) uniquely.

## APPENDIX

### THE AFFECT OF SMALL NUMBER ON KOLMOGOROV-SMIRNOV (K-S) TWO-SAMPLE TESTS

As discussed in Chapter 4, the two-sample Kolmogorov-Smirnov (K-S) test (Press et al. 1992) is a test that returns a probability (p-value) of two separate distributions being statistically consistent with being drawn from the same parent distribution. In this study, the p-value was used to prove (to some significance) that the distribution of WISE AGNs/Ext. WISE AGNs is statistically different from other mergers and interactions in terms of a given property. For example, a p-value of 0.05 for a given property would suggest that, to 95 percent confidence, the subset of WISE AGNs/Ext. WISE AGNs is statistically different from that of Region C, and thus the WISE AGN merging and interacting subset is unique from other mergers and interactions in terms of that property.

To quantify the affect of our small sample size on the K-S test p-values, we perform a series of K-S tests on randomly generated Gaussian distributions for stellar mass (see Chapter 4.1). Examples of these distributions are shown in Figure 20. We create two large samples with 1000 data points each: one with an average value of 10.75 (shown in blue), one with an average value of 11.25 (shown in green). We chose both distributions to have a one-sigma value of one unit. The close choice of average ensures an overlapping distribution, similar to the distributions of our subsamples in Chapter 4. For our small-number samples, we created Gaussians with 61 (red) and 22 (aqua) points with the same average value as the first large distribution (10.75).

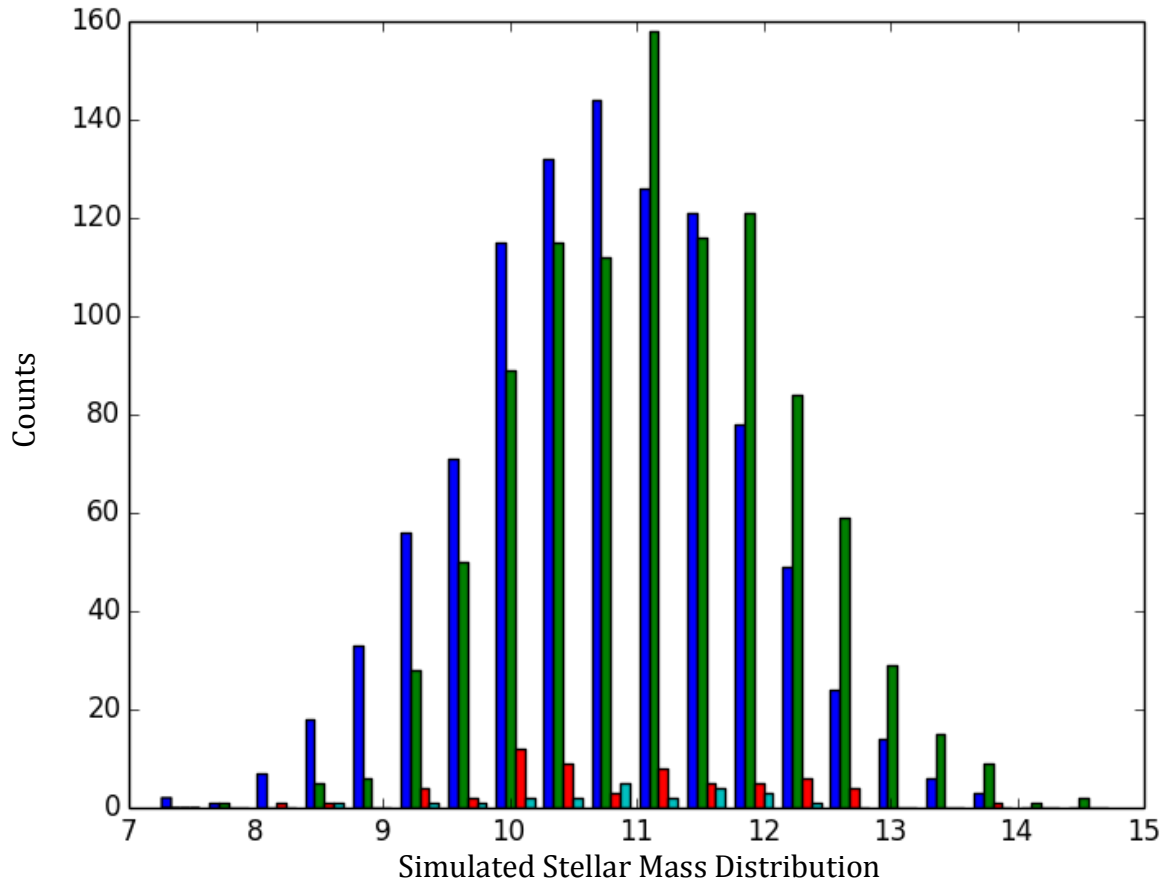


Figure 20. Sample of Gaussian Distributions Used to Quantify the Affect of Small Numbers on K-S Test p-values

*Notes.* Sample of Gaussian distributions with varying number of data points contained: the blue and green distributions each have 1000 points, the red distribution has 61 points (to simulate our Extended WISE AGN population in Chapter 4), and the aqua distribution has 22 points (to simulate our WISE AGN population in Chapter 4). The blue, red, and aqua distributions all have an average value of 10.75. The green distribution has an average value of 11.25. All Gaussians are given one-sigma values of one unit.

We first perform K-S tests for the distributions we chose to be the same: all distributions with a mean value of 10.75. This includes one distribution with 1000 points (shown in blue above), one distribution with 61 points (shown in red above and chosen to simulate our Extended WISE AGN population), and one distribution with 22 points (shown in aqua above and chosen to simulate our WISE AGN population). We compare our two

smaller distributions to the larger distribution, as we did in Chapter 4. Because we chose these distributions to be centered on the same mean value, we should expect p-values consistent with the distributions being drawn from the same parent distribution (above 0.05). To minimize the affect of a random Gaussian distribution, we perform the K-S tests 1000 times with a different set of distributions each time and plot the p-values in Figure 21.

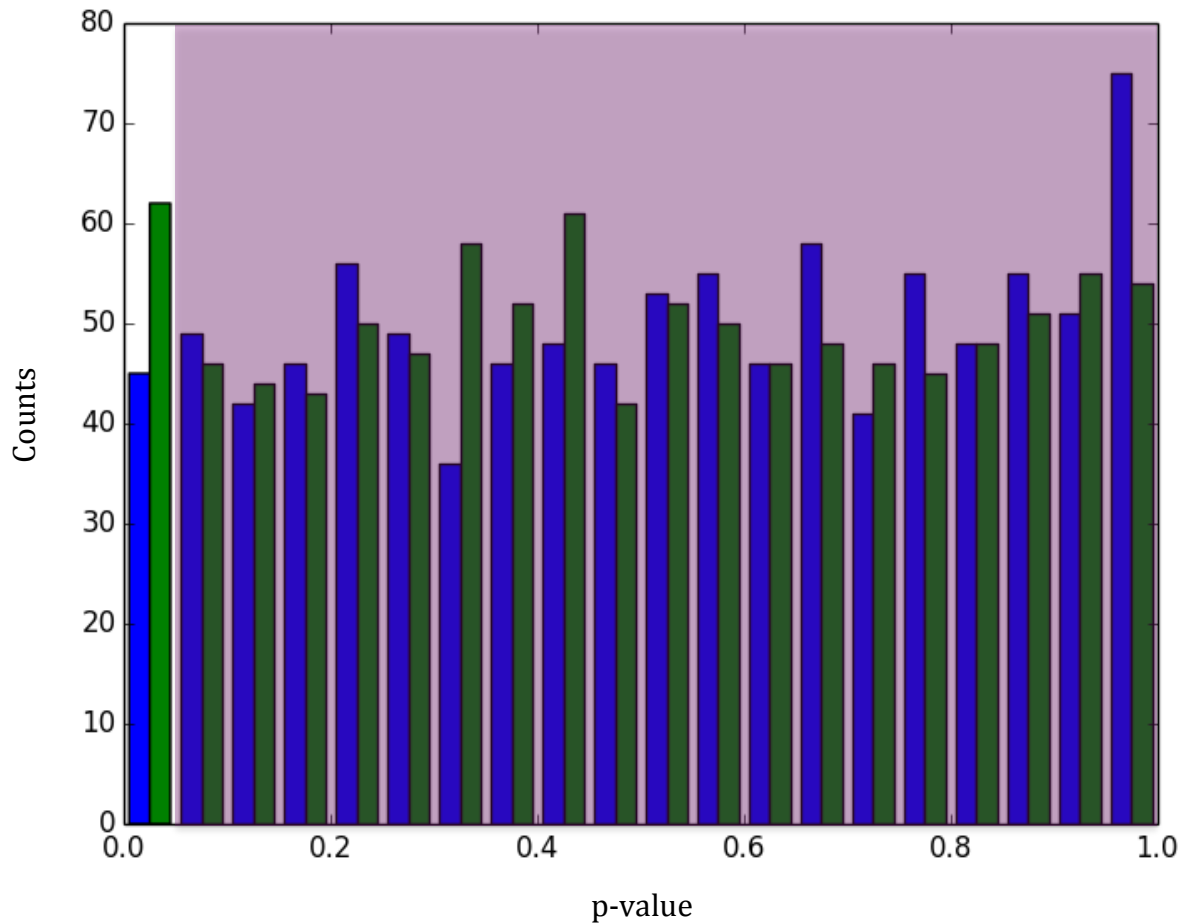


Figure 21. Distributions of p-values for Similar Distributions

*Notes.* Distribution of 1000 K-S test p-values for randomly generated Gaussian distributions with the same selected mean value. Blue represents the p-values of comparing the distribution of 61 points to the full distribution (1000 points). Green represents the p-values of comparing the distribution of 22 points to the full distribution. The purple shaded region shows the region of the figure that is consistent with the distributions being drawn from the same parent sample, as we would expect.

As shown in the figure, the likelihood of the K-S test returning a p-value consistent with distributions being from the same parent sample (shown as the shaded purple region) is  $\sim 95$  percent for both sized distributions. This implies that, for distributions that are statistically equivalent, small numbers should not affect the K-S test p-value.

Next, we test the affect of small numbers on the K-S test p-value for differing distributions. To do this, we make three K-S test comparisons: (1) the full 1000-point distribution with a mean value of 10.75 to the full 1000-point distribution with a mean of 11.25, (2) the 61-point distribution with a mean value of 10.75 to the full 1000-point distribution with a mean of 11.25, and (3) the 22-point distribution with a mean value of 10.75 to the full 1000-point distribution with a mean of 11.25. Again, we minimize the affect of random Gaussian distributions by performing the K-S tests 1000 times with a different set of distributions each time. The p-value distribution for these tests is shown in Figure 22. As shown in the figure, the likelihood of the K-S tests returning a p-value consistent with distributions being from the different parent samples (shown as the shaded purple region) drops with decreasing sample size. For the sample of only 22 data points (similar to our WISE AGN population in Chapter 4), the likelihood of the p-value reflecting the difference in distributions ( $p\text{-value} < 0.05$ ) is only  $\sim 50$  percent. The remaining  $\sim 50$  percent of the time, the K-S test returns a value consistent with the distributions being drawn from the same parent sample, despite having different mean values. This implies that small numbers can drastically skew the results of the K-S test for distributions that are statistically different, but occupy the same space.



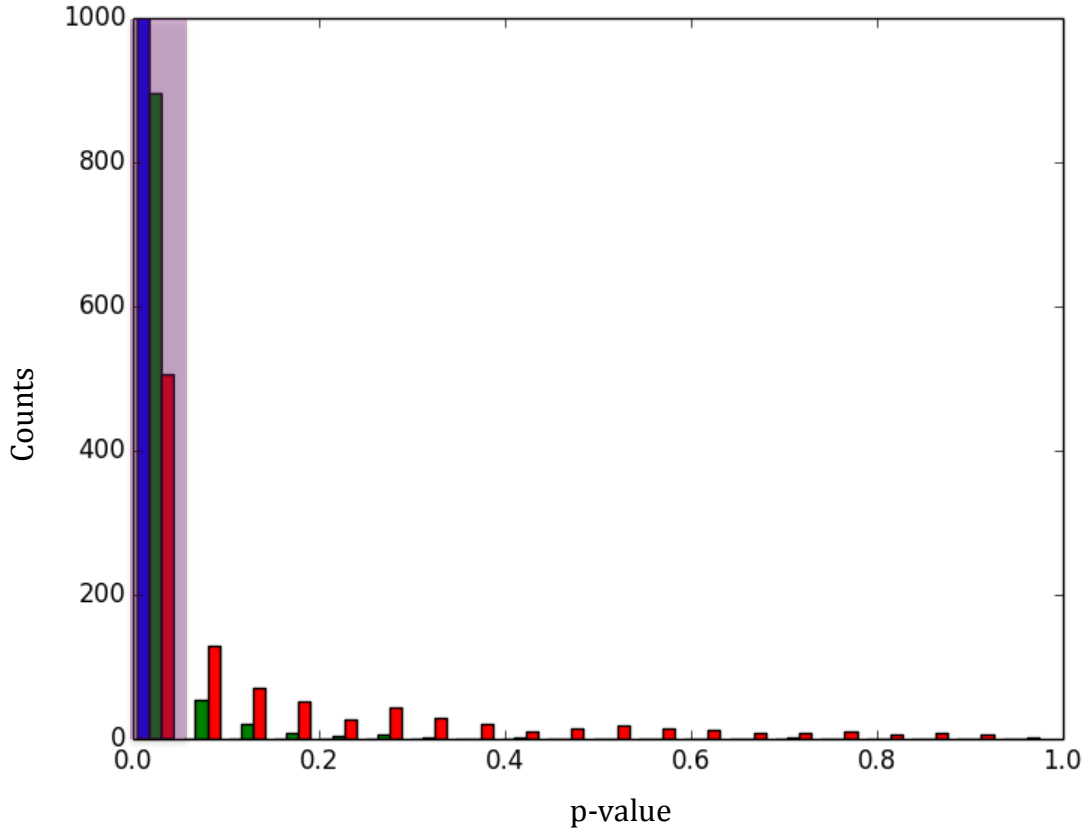


Figure 22. Distributions of p-values for Different Distributions

*Notes.* Distribution of 1000 K-S test p-values for randomly generated Gaussian distributions with different mean values. Blue represents the p-values of comparing the distribution of 1000 points with mean value 10.75 to the full distribution (1000 points) with mean value 11.25. Green represents the p-values of comparing the distribution of 61 points with mean value 10.75 to the full distribution (1000 points) with mean value 11.25. Red represents the p-values of comparing the distribution of 61 points with mean value 10.75 to the full distribution (1000 points) with mean value 11.25. The purple shaded region shows the region of the figure that is consistent with the distributions being drawn from different parent samples, as we would expect.

With the results shown in Figures 21 and 22, we conclude that the K-S test is sufficient at detecting differing distributions for the small number sample we use in Chapter 4 (with 95% confidence for p-values less than 0.05). However, we find that there's a high probability for our sample of 22 WISE AGNs for the K-S test to be consistent with the distributions being drawn from the same parent sample despite being statistically different.

## REFERENCE LIST

- Adelman-McCarthy, J. K. et al., 2006, *The Astrophysical Journal Supplement Series*, 162, 38
- Alonso, M. S., Tissera P. B., Coldwell G., & Lambas D. G., 2004, *Monthly Notices of the Royal Astronomical Society*, 352, 1081
- Ashby, M. L. N. et al., 2009, *The Astrophysical Journal*, 701, 428
- Assef, R. J. et al., 2013, *The Astrophysical Journal*, 772, 26
- Baldwin, J. A., Phillips M. M., & Terlevich R., 1981, *Publications of the Astronomical Society of the Pacific*, 93, 5
- Barnes, J. E., 2002, *Monthly Notices of the Royal Astronomical Society*, 333, 481
- Barton, E. J., Geller M. J., & Kenyon S. J., 2000, *The Astrophysical Journal*, 530, 660
- Baugh, C. M., Cole S., & Frenk C. S., 1996, *Monthly Notices of the Royal Astronomical Society*, 283, 1361
- Bell, E. F., McIntosh D. H., Katz N., & Weinberg M. D., 2003, *The Astrophysical Journal Supplement Series*, 149, 289
- Best, P. N. et al., 2005, *Monthly Notices of the Royal Astronomical Society*, 362, 25
- Blanton, M. R. et al., 2003, *Astronomical Journal*, 125, 2276
- Blanton, M. R. et al., 2005, *Astronomical Journal*, 129, 2562
- Brinchmann, J. et al., 2004, *Monthly Notices of the Royal Astronomical Society*, 351, 1151
- Brodwin, M. et al., 2014, *The Astrophysical Journal*, 779, 138
- Capelo, P. R. et al., 2014, *Monthly Notices of the Royal Astronomical Society*, 447, 2123
- Cisternas, M. et al., 2011, *The Astrophysical Journal*, 726, 57
- Clemens, M. S. et al., 2013, *Monthly Notices of the Royal Astronomical Society*, 433, 695

- Cole, S., Lacey C. G., Baugh C. M., & Frenk C. S., 2000, *Monthly Notices of the Royal Astronomical Society*, 319, 168
- Cotini, S. et al., 2013, *Monthly Notices of the Royal Astronomical Society*, 431, 2661
- Cox, T. J. et al., 2008, *Monthly Notices of the Royal Astronomical Society*, 384, 386
- Davis, M., Efstathiou G., Frenk C. S., & White S. D. M., 1985, *The Astrophysical Journal*, 292, 371
- DeBuhr, J., Quataert E., & Ma C.-P., 2011, *Monthly Notices of the Royal Astronomical Society*, 412, 1341
- Dekel, A. & Birnboim Y., 2006, *Monthly Notices of the Royal Astronomical Society*, 368, 2
- Di Matteo, T., Springel V., & Hernquist L., 2005, *Nature*, 433,604
- Donoso, R. et al., 2012, *The Astrophysical Journal*, 748, 80
- Donoso, E., Yan L., Stern D., & Assef R. J., 2014, *The Astrophysical Journal*, 789, 44
- Ellison, S. L., Patton D. R., Simard L., & McConnachie A. W., 2008, *Astronomical Journal*, 135, 1877
- Ellison, S. L., Patton D. R., Mendel J. T., & Scudder J. M., 2011, *Monthly Notices of the Royal Astronomical Society*, 418, 2043
- Ellison, S. L., Mendel J. T., Patton D. R., & Scudder J. M., 2013, *Monthly Notices of the Royal Astronomical Society*, 435, 3627
- Fan, L. et al., 2014, *The Astrophysical Journal*, 784, 9
- Gorjian, V. et al., 2008, *The Astrophysical Journal*, 679, 1040
- Goulding, A. D. & Alexander D. M., 2009, *Monthly Notices of the Royal Astronomical Society*, 398, 1165
- Goulding, A. D. et al., 2011, *Monthly Notices of the Royal Astronomical Society*, 411, 1231

Goulding, A.D. et al., 2012, *The Astrophysical Journal*, 755, 5

Granato, G. L. et al., 2004, *The Astrophysical Journal*, 600, 580

Gruppioni, C., Pozzi F., Zamorani G., & Vignali C., 2011, *Monthly Notices of the Royal Astronomical Society*, 416, 70

Gürkan, G., Hardcastle M. J., & Jarvis M. J., 2014, *Monthly Notices of the Royal Astronomical Society*, 438, 1149

Hann, S. et al., 2009, *The Astrophysical Journal*, 692, 1623

Heckman, T. M. et al., 2004, *The Astrophysical Journal*, 613, 109

Hickox, R. et al., 2014, *The Astrophysical Journal*, 782, 9

Holden, B. P., van der Wel A., Rix H.-W., & Franx M., 2012, *The Astrophysical Journal*, 749, 96

Hopkins, P. F. & Elvis M., 2010, *Monthly Notices of the Royal Astronomical Society*, 401, 7

Hopkins, P. F. et al., 2006, *The Astrophysical Journal Supplement Series*, 163, 1

Hopkins, P. F., Hernquist L., Cox T. J., & Kereš D., 2008, *The Astrophysical Journal Supplement Series*, 175, 356

Hopkins, P. F., Cox T. J., Younger J. D., & Hernquist L., 2009, *The Astrophysical Journal Supplement Series*, 691, 1168

Jarrett, T. H. et al., 2011, *The Astrophysical Journal*, 735, 112

Karouzos, M. et al., 2010, *Astronomy & Astrophysics*, 519, 62

Karouzos, M., Jarvis M. J., & Bonfield D., 2014, *Monthly Notices of the Royal Astronomical Society*, 439, 861

Kauffmann, G. & Haehnelt M., 2000, *Monthly Notices of the Royal Astronomical Society*, 311, 576

Kauffmann, G., White S. D. M., & Guiderdoni B., 1993, *Monthly Notices of the Royal Astronomical Society*, 264, 201

Kauffmann, G. et al., 2003, *Monthly Notices of the Royal Astronomical Society*, 346, 1055

Kaviraj, S., Schawinski K., Silk J., & Shabala S. S., 2011, *Monthly Notices of the Royal Astronomical Society*, 415, 3798

Kennicutt, R. C., Jr, 1998, *Research in Astronomy & Astrophysics*, 36, 189

Kennicutt, R. C., Jr, et al., 1987, *The Astronomical Journal*, 93, 1011

Kereš, D., Katz N., Weinberg D. H., & Davé R., 2005, *Monthly Notices of the Royal Astronomical Society*, 363, 2

Kewley, L. J. et al., 2001, *The Astrophysical Journal*, 556, 121

Lake, G. & Dressler A., 1986, *The Astrophysical Journal*, 219, 46

Lambas, D. G., Tissera P. B., Alonso M. S., & Coldwell G., 2003, *Monthly Notices of the Royal Astronomical Society*, 346, 1189

Lotz, J. M., Jonsson P., Cox T. J., & Primack J. R., 2010, *Monthly Notices of the Royal Astronomical Society*, 404, 590

Mateos, S. et al., 2012, *Monthly Notices of the Royal Astronomical Society*, 426, 3271

McIntosh, D. H. et al., 2008, *Monthly Notices of the Royal Astronomical Society*, 388, 1537

McIntosh, D. H. et al., 2014, *Monthly Notices of the Royal Astronomical Society*, 442, 533

McIntosh, D. H. et al., in preparation, University of Missouri – Kansas City

Nazaryan, T. A. et al., 2014, *International Astronomical Union Symposia*, 304, 327

Nicastro, F., Fiore F., & Matt G., 1999, *The Astrophysical Journal*, 517, 108

Patton, D. R. et al., 2013, *Monthly Notices of the Royal Astronomical Society*, 433, L59

Press, W. H., W. T. Vetterling, S. A. Teukolsky, & B. P. Flannery, *Numerical Recipes in Fortran 77*. New York, NY: Press Syndicate of the University of Cambridge, 1992.

Rosario, D. J. et al., 2015, *Astronomy & Astrophysics*, 573, 85

Rothberg, B. & Joseph R. D., 2006, *The Astronomical Journal*, 131, 185

Ryden, B., *Introduction to Cosmology*. San Francisco, CA: Pearson Education Inc., 2003.

Sabater, J., Best P. N., & Argudo-Fernandez M., 2013, *Monthly Notices of the Royal Astronomical Society*, 430, 638

Satyapal, S. et al., 2014 *Monthly Notices of the Royal Astronomical Society*, 441, 1297

Schawinski, K. et al., 2007, *Monthly Notices of the Royal Astronomical Society*, 382, 1415

Schawinski, K. et al., 2009, *The Astrophysical Journal*, 69, L19

Scott, C., & Kaviraj S., 2014, *Monthly Notices of the Royal Astronomical Society*, 437, 2137

Shao, L. et al., 2013, *Monthly Notices of the Royal Astronomical Society*, 436, 3451

Shier, L. M., & Fischer J., 1998, *The Astrophysical Journal*, 497, 163

Springel, V., & Hernquist L., 2005, *The Astrophysical Journal*, 622, L9

Springel, V., Mateo T. D., & Hernquist L., 2005, *Monthly Notices of the Royal Astronomical Society*, 361, 776

Stern, D. et al., 2005, *The Astrophysical Journal*, 631, 163

Stern, D. et al., 2012, *The Astrophysical Journal*, 753, 30

Storchi-Bergman, T. et al., 2001, *The Astrophysical Journal*, 559, 147

Strauss, M. A. et al., 2002, *The Astronomical Journal*, 124, 1810

Thacker, R. J., MacMackin C., Wurster J., & Hobbs A., 2014, *Monthly Notices of the Royal Astronomical Society*, 443, 1125

Toba, Y. et al., 2014, *The Astrophysical Journal*, 788, 45

- Treister, E., Schawinski K., Urry C. M., & Simmons B. D., 2012, *The Astrophysical Journal*, 758, 39
- Villforth, C. et al., 2014, *Monthly Notices of the Royal Astronomical Society*, 439, 3342
- Volonteri, M., Haardt F., & Madau P., 2003, *The Astrophysical Journal*, 582, 559
- White, S. D. M. & Rees M. J., 1978, *Monthly Notices of the Royal Astronomical Society*, 183, 341
- Wright, E. L. et al., 2010, *The Astronomical Journal*, 140, 1868
- Yan, D. et al., 2006, *The Astrophysical Journal*, 648, 281
- Yan, L. et al., 2013, *The Astronomical Journal*, 145, 55
- Yang, X. et al., 2007, *The Astrophysical Journal*, 671, 153
- Zolotov, A. et al., 2014, arXiv:1412.4783

## VITA

Madalyn Elizabeth Weston was born on December 19, 1989, in Independence, Missouri. She was educated in the Independence Public School District and graduated from William Chrisman High School in 2008. She received the A+ Scholarship to attend the Kansas City Metropolitan Community College system, and transferred to Missouri University of Science and Technology to finish her Bachelor of Science degree in Physics in 2012. While at Missouri S&T, she worked for the university in a solid-state physics lab with Dr. Yew San Hor.

After receiving her Bachelor of Science degree, Ms. Weston continued her education at the graduate level at the University of Missouri – Kansas City. She accepted a research position with Dr. Daniel McIntosh, analyzing merging and interacting galaxies using data from the NASA WISE telescope, the Sloan Digital Sky Survey (SDSS) and GALEX. While working under Dr. McIntosh, Ms. Weston attended two American Astronomical Society meetings, three Mid-American Regional Astrophysics Conferences, the Missouri Space Grant Conference, and the WISE @ 5 Conference at Caltech in Pasadena, California. Upon completion of her degree requirements, Ms. Weston plans to begin a career in science education.